

Abstract I consider the microscopic mechanisms by which a particular left-right (L/R) asymmetry is generated at the organism level from the microscopic handedness of cytoskeletal molecules. In light of a fundamental symmetry principle, the typical pattern-formation mechanisms of diffusion plus regulation cannot implement the “right-hand rule”; at the microscopic level, the cell’s cytoskeleton of chiral filaments seems always to be involved, usually in collective states driven by polymerization forces or molecular motors. It seems particularly easy for handedness to emerge in a shear or rotation in the background of an effectively two-dimensional system, such as the cell membrane or a layer of cells, as this requires no pre-existing axis apart from the layer normal. I detail a scenario involving actin/myosin layers in snails and in *C. elegans*, and also one about the microtubule layer in plant cells. I also survey the other examples that I am aware of, such as the emergence of handedness such as the emergence of handedness in neurons, in eukaryote cell motility, and in non-flagellated bacteria.

Keywords Cytoskeleton; motor proteins; actin; chirality; handedness

PACS PACS 87.19.l, 87.16.Ka, 87.16.Nn, 87.17.Ee

Christopher L. Henley

Possible origins of macroscopic left-right asymmetry in organisms

subtitle here

Received: date / Accepted: date

1 Introduction

Most animals – and many plants – have systematic chiral asymmetries, uniform throughout their species. Yet pattern-formation in development is based on reaction-diffusion equations – where “reaction” includes the rate equations of gene regulation and expression – and perhaps on elasticity. But diffusion and elasticity, being described physically by symmetric tensors, are not chiral; the chiral information must somehow be brought from the molecular scale to the macroscopic scale. It is reminiscent of Feynman’s fantasy of how one could communicate the absolute definitions of left and right to extraterrestrials purely by radio: they can perform particle physics experiments that access the inherent left-right asymmetry of physics on the subatomic scale. To achieve a systematic handedness, every embryo must analogously perform an experiment that accesses the left-right asymmetry of biochemistry at the molecular scale. Embryologists have recognized this as a fundamental question over the past 25 years [1, 2, 3, 4].

Why is handedness an attractive topic for theoretical modeling, and why should it be claimed by physics? In the first place, unlike most pattern-forming instabilities in development, handedness is a choice between *equivalent* outcomes and is hence more clearcut to study [5]. In other words it is a *symmetry breaking*, akin to that in the Ising model of statistical physics. Being binary also makes it amenable to typical biological experiments, where the outcomes are classified qualitatively. And *symmetry* puts constraints on

F. Author
first address
Tel.: +123-45-678910
Fax: +123-45-678910
E-mail: fauthor@example.com

S. Author
second address

the conceivable mechanisms, giving the theorist a rare opportunity to make *a priori* statements about biology.

Secondly, it appears that the mechanisms involve *physics* in a central fashion: forces and motions in the cytoskeleton. Now, most stories in biology are about *signaling* and it is natural that biologists look for signal-based mechanisms. Signal-based pattern formation requires two ingredients: (1) gene regulation or other reactions, and (2) transport of signaling molecules by diffusion, or by active transport that similarly just depends on proximity. The diffusion ingredient is responsible for the spatial patterning, but *it cannot produce an L/R spatial patterning*, since diffusion does not distinguish handedness (see Sec. 1.3.2). The actual mechanisms, insofar as we know them, involve literal *forces* or *torques* exerted by molecular motors, acting along the *cytoskeleton* of stiff, semi-macroscopic fibers, and in this sense the topic belongs to mechanics.

This paper (superseding Ref. [6]) is a review of sorts, but not mainly of theoretical results (which are few). Instead, it aims to survey diverse systems manifesting left/right asymmetries, with the aim of finding commonalities and classifying the differences usefully. The hope is that – since the mechanism is strongly constrained by symmetry – one can exhaustively categorize the models and that this catalog will be helpful in finding the right model for each system. What is actually done here is to lay out the facts for the most promising systems and attempt to imagine all the plausible models for each, as groundwork for future modeling work (or as motivation for new experiments needed before we can estimate basic parameters in the models). The specific hypothetical proposals sketched are my own, except where previous work is mentioned and cited. What is probably most novel here is to consider how the handedness may realistically be implemented at the molecular level in specific cases; the more physical ideas in past discussions have mostly been at the more macroscopic level of mechanics. The most penetrating existing thoughts about mechanical (but not molecular) mechanisms are found in Wood’s review [2].

Note that the question of this paper is quite separate from another one that has long attracted physicists, the way organic molecules originally broke left-right symmetry in prebiotic evolution [7,8]

1.1 Outline of paper and list of examples

The paper begins (the rest of Section 1) by laying out the necessary properties of left/right mechanisms (along with some assumptions I will adopt). Furthermore it lays out the important categories: spontaneous instability (=symmetry breaking) versus proportionate response (Subsec. 1.5), cell level versus multicellular level (Subsec. 1.2), screw versus anchoring-molecule mechanisms (Subsec. 1.4), and single-unit versus collective mechanisms.

After that, the sections run through the major experimental examples of L/R asymmetry, which I will now preview in order.

1.1.1 Example: vertebrates and cilia-driven flow

The best-known left-right asymmetry is the internal organs (viscera) of vertebrates [9,10] – among humans, [11] just $\sim 10^{-4}$ of us have mirror-reversed insides (so that the heart is on the right side). Most vertebrate studies use one of four model systems: mouse, chick, *Xenopus* frog, or zebrafish.

In 1998, it was observed through video imaging that (at one stage) the surface of the mouse embryo has cells with cilia whose tips move *circularly* in a clockwise sense, [12,14] which breaks the symmetry sufficient to drive a leftwards flow in the surrounding fluid [13]. If some (yet undiscovered) chemical signal is emitted, it will be preferentially carried to the left and distinguish that side, so the cilia-driven flow is clearly *sufficient* to trigger handedness. Indeed, in one experiment that reversed the flow in a few embryos, they subsequently developed in a mirror reversed form [15].

This is the accepted picture, but subsequent studies have complicated it: e.g., in the zebrafish, the cilia are on the internal surface of an enclosed sphere, called Kupfer’s vesicle, and a different version of the fluid dynamics story will be called for. More importantly, left/right asymmetries are reported in vertebrates long *before* the cilia start moving, in the form of a polarization of the gap junctions connecting cells, leading to ion flow [3,16]. Thus cilia do not *necessarily* determine handedness; indeed a non-cilia mechanism is claimed to determine the body asymmetry in the case of *Xenopus* frogs [17, 18].

In this paper, I will skip the often-told story of vertebrates and focus on other examples for which their microscopic physical mechanisms have not even been proposed, let alone accepted.

1.1.2 Example: molluscs and *C. elegans*

Another long-known example is the chirality of mollusc shells, which has been studied in many species, most of which are dominantly right-handed (reversal frequency $\sim 10^{-4}$). And even the tiny *C. elegans* nematode “worm” has L/R asymmetry [2,4,19,20], most significantly in the left and right copies of a certain chemosensing neuron.

In both molluscs and *C. elegans*, a twist in the positioning of cells during the first three divisions determines the embryo’s handedness. This seems to be due to the chiral dynamics of an actin-myosin layer associated with the membrane. In sec. 2, I will walk in some detail through three levels of description, proposing some physics on each level. This is the most important section of this paper. These stories are not quantitative, but they do lead to clear predictions of the *sign* of handedness in various phenomena.

1.1.3 Example: cortical microtubules in plant cells

There is a surprisingly similar story of handedness in plants (Sec. 3), often manifested by roots and shoots taking helical paths – e.g. the twining of vines – with a species-dependent handedness. At the microscopic level, plant cells develop an array of parallel microtubules along the membrane, which

has some twist around the cylindrical cell's long axis. This is believed to determine the sense of macroscopic helical behaviors. A couple of mechanisms will be sketched in Sec. 3 for the way that the array gets aligned helically.

1.1.4 Example: nerve cells and brain handedness

Section 4 gathers several examples related to motility and/or intercellular forces. The most interesting of these is the human brain: we show right hand dominance as a side effect of left brain dominance [?,21]. The brain handedness probably has a different mechanism from the viscera, since it is observed to be *independent* of the handedness of internal organs [3,9,11], and is less reliable by a factor of 1000 (1/10 of us are right-brain-dominant). It is unclear whether the brain asymmetry other animals is related to ours [22,23]; in the case of zebrafish, it seems to just follow the handedness of internal organs [24].

To relate the macroscopic level to lower ones, we note that nerve tissue forms by migration of nerve cells and by the growth of very long axons (or dendrites). Growing axons indeed are observed to turn chirally, reminiscent of plant roots [?].

Both migration and growth dynamics depend on the cell extending pseudopods, that are driven by actin polymerization forces in the bulk. Therefore, I outlined a (highly speculative) mechanism based on actin polymerization (Sec. 4.2). I have lumped in the recent discovery of chiral asymmetries in the motility of (non-nerve) mammalian cells (Sec. 4.3) and in the gut tissues of flies (Sec. 4.4).

1.1.5 Bacteria

For completeness and because their handedness is to some degree understood, I include bacteria in the story (Sec. 5). The interesting case is when handedness is determined by the bacterial cytoskeleton (Sec. 5.2).

1.2 Cell level and multicellular level stories

Any example of L/R specification requires explanations on (at least) two levels. The *cell level* story takes us from molecules to handed behavior at the level of the entire cell. This typically emerges from some collective state of the cytoskeleton, which can be modeled in the framework of non-equilibrium statistical mechanics. The *multicellular level* story starts from the cell behavior and explains how this specifies a macroscopic handedness in the whole embryo (or plant), typically in the framework of solid mechanics. A sort of multiscale modeling is called for, meaning we not only have a theory for each level, but also can numerically compute the parameters governing one level from the parameters of the level below it.

In the case of the circularly moving cilia that affect handedness in the mouse and other vertebrates (Sec. 1.1.1) the cell level story is merely the growth of one cilium containing dynein molecules connecting microtubule

pairs in a clockwise direction, as viewed from above. The multicellular level story involves not solid but fluid mechanics in this case [13] (the exterior fluid flow driven by cilia).

1.3 Symmetry constraints and basic assumptions

In this subsection, I want to identify necessary ingredients in a left/right mechanism; I argue that basic symmetry and statistical mechanics put *a priori* constraints on what can work.

1.3.1 Pre-existing axes and two-dimensionality

Any organism can develop mutually orthogonal axes $\hat{\mathbf{z}}$, $\hat{\mathbf{x}}$, and $\hat{\mathbf{y}}$, through a combination of reaction and diffusion by chemical signals. In an embryo, $\hat{\mathbf{x}}$ might represent the *anterior/posterior* (A/P) axis and $\hat{\mathbf{z}}$ might represent the *dorsal/ventral* (D/V) axis; within a single cell, $\hat{\mathbf{x}}$ might represent a direction of polarization and $\hat{\mathbf{z}}$ might represent the normal to the membrane. The problem is how to ensure the third axis satisfies a “right-hand rule”

$$\hat{\mathbf{y}} = \hat{\mathbf{z}} \times \hat{\mathbf{x}} \quad (1)$$

rather than its opposite.

A key observation [6] is that symmetry requires that *each of the three symbols* on the right-hand side of (1) has a *specific physical (biological) correlate* which is part of the mechanism: i.e., two kinds of preexisting polarization representing $\hat{\mathbf{x}}$ and $\hat{\mathbf{z}}$, and something chiral representing the “ \times ” in (1). The above symmetry principle applies at *each* of the levels distinguished in Sec. 1.2. At the bottom level, the chiral element is obviously the microscopic chirality of molecules, under genetic control, which can enter in a couple of ways (see Sec. 1.4).

The above observation may appear trivial, but it has a less trivial corollary. The commonest situation in which *two* kinds of pre-existing polarization are present is a *planar* geometry such that “up” and “down” directions are inequivalent, so the $\hat{\mathbf{z}}$ is the unit normal to that plane. On the cell level such a plane is the *membrane*; on the organism level, it means the mechanism should operate at a stage during development when the embryo is still roughly planar in shape. It seems harder to implement handedness inside a three-dimensional bulk, and I do not know of a plausible such mechanism in any system.

1.3.2 “Hall effect” in diffusion?

Development is governed normally by *reactions* and *diffusion*. Here “reactions” includes regulation of DNA transcription and translation to proteins. Diffusion usually means a chemical species is produced by some cells and diffuses to others (either in the intercellular medium, or via a network of gap junctions linking neighboring cells). A nonzero net transport emerges statistically from local steps that appear rather random.

It would be amusing (but wrong) if the chiral bias could emerge via the diffusion analog of the Hall effect (of electrical conduction in magnetic fields). The usual Fick's law for the diffusion current reads

$$\mathbf{j} = -D\nabla\rho \quad (2)$$

where ρ is the number density. In the presence of chiral scatterers, do we get another term proportional to $\hat{z} \times \nabla\rho$, for some axis \hat{z} , so that the current deviates by some regular angle from the concentration gradient? The answer is no: diffusion in equilibrium satisfies time reversal symmetry, whereas such a "Hall effect" violates time reversal symmetry. I suspect it can be proven that the "Hall" bias is negligible so long as the work done during a velocity correlation time is small compared to a thermal energy $k_B T$; it would be an interesting challenge to turn that into a theorem.

Such a theorem need not apply to cytoskeletal dynamics, since the motions of motor molecules and the polymerization of fibers are far from equilibrium processes. Furthermore, the motion of a motor or the growth state of a fiber tends to persist for many steps, ensuring a long velocity correlation time. For these reasons, I will consider only cytoskeletal-based mechanisms. That seems to be the expectation of biologists also, presumably because cytoskeletal dynamics is the normal way to generate asymmetries such a polarization in a cell; also, in all particular examples for which we have partial experimental information, the mechanism does seem to be cytoskeletal.

1.4 Filament screw or membrane-anchoring mechanism?

There are two broad classes of mechanism [6] that can implement chirality on the microscopic (cell) level. First, a *screw mechanism* is one depending on conversion between longitudinal and rotational motion, due to the inherent helicity of an actin filament or a microtubule. ("motion" usually refers to a translocating motor, but could instead be the fiber's growth, e.g. the microtubule screw-ratchet mechanism (Sec. 3.4) and/or mere elastic displacement of its tip, e.g. in actin polymerization (Sec. 4.2).

Some screw mechanisms – all of them conjectural –

- (a) actomyosin chirality arising from the azimuthal component of myosin power strokes (Sec. 2.4);
- (b) a helical Brownian ratchet in microtubule collisions (Sec. 3.4);
- (c) the change in pitch of actin fibers due to a change in their longitudinal load (Sec. 4.2).
- (d) a pedagogical example (conceivably related to *Drosophila*, Sec. 4.4) whereby a processive motor that moves on its fiber with a helical bias (e.g. Myosin V) in the steady state tends to pull a cargo on the "right hand side of the road", see Ref. [6], Sec. 3.1.
- (e) the non-biological conversion mechanism in Ref. [25], whereby microtubules sliding on a kinesin-coated surface tend to bend to the left.

The second route to implement chirality is that a specific linking molecule binds to the fibers with a rigid orientation. and is anchored in the membrane, hence I call it an "anchoring" mechanism.

Some examples of anchoring mechanisms are

- (a) the branching of microtubules in plant cell (Sec. 3.2, below);
- (b) the correct growth of a cilium out of a cell, in the nodal cilia mechanism for vertebrates;
- (c) the conjectured kinked-attachment mechanism inducing a fiber to spiral with a particular pitch inside a cylindrical cell (Sec. 3.5).

If a membrane-anchoring mechanism is involved, this furnishes a hint to biologists who hunt for pertinent genes using genetic engineering or by screening for aberrant phenotypes following mutagenesis.

Screw mechanisms, as they depend directly on helical symmetry, appear more elegant in the context of physics. By contrast, the anchoring mechanisms appear more natural in the context of molecular biology. Underlying the screw/anchor dichotomy is one between two kinds of chirality: (1) *absolute* – the direct fixing of a third axis, which realizes the absolute kind of chirality; (2) *relative* – the sign of a rotation relating two directions, which is realized by the screw motion. Indeed, the screw situation preserves rotational symmetry around the axis, as well as translation along it; axes are fixed indirectly, perhaps at the intercellular scale. The respective collective dynamic states described here, for both actomyosin in animal cells and for cortical microtubule arrays in plant cells, realize “relative” chirality on a larger scale. In either case, up/down asymmetry (with respect to the membrane normal) becomes converted to a chiral asymmetry within the layer.

A related but distinct dichotomy is that chirality may be implemented either through static positioning in the system, or else in its dynamics. Thus the attachment type scenario, realized when the interacting molecules have a unique bonding site, is not just absolute but static; by contrast, in the screw scenario the binding is to a polymer with many symmetry-equivalent binding sites, so this is not only relative but dynamic.

It will be seen that a third combination is possible in principle, relative and static. Such a situation is realized when parallel, microscopically helical fibers aggregate in an array with a cross-section that is (approximately) a triangular lattice. As analyzed in Ref. [26], adjacent fibers “want” to be rotated slightly about the line connecting them – this is the same generic asymmetry responsible for cholesteric liquid crystals. Hence it turns the fibers form bundles of a parameter-dependent size, each of which is a sort of twisted rope. The continuum elasticity of this complex liquid crystal phase will be chiral too (in the “relative” sense). If cells were filled with such domains, their passive mechanical chirality could be *part* of a mechanism to implement chirality at the inter-cellular level. However, the only biologically pertinent example I know of such an array is the coiling of viral DNA inside phase capsids¹

1.5 Spontaneous symmetry breaking?

Another dichotomy in the scenario is whether or not a robust *spontaneous* symmetry breaking underlies the chirality. Here, “symmetry breaking” refers

¹ A “phage capsid” is the protein container of a virus that infects bacteria

that a definite orthogonal axis is produced in (1), but with a random sense, so that left- and right-handed individuals are equally likely. The systematic handedness is then controlled by an *independent* mechanism that supplies a *small* chiral biasing field. This is analogous, in statistical mechanics, to the small magnetic field which determines the magnetization sense of an Ising magnet quenched into its *ferromagnetic* phase.

The alternative to spontaneous symmetry breaking may be called a “linear response” scenario. In this case, our system is the analog of the *paramagnetic* state in statistical mechanics. The left-right asymmetry is a smooth function of the chiral bias strength, and linearly proportional to it if it is small. It follows that wild-type chiral bias must be larger in the “linear response” scenario than in the symmetry-breaking one. The “linear response” regime can be recognized biologically because a mutant missing the chiral bias remains symmetric and does not form a third axis in either direction.

In the rest of the paper, except where noted, I implicitly assume the symmetry-breaking scenario. This means that the sought-for mechanism need only produce a weak bias (let’s arbitrarily say $\sim 10^{-2}$), since its effects get amplified hugely by the (incipient) long range order. A mutant missing the chiral bias forms a third axis just as well as the wild type, except the sign of \hat{y} is randomized. The latter phenomenon is seen in human beings with Kartagener’s syndrome (missing a certain variety of the molecular motor dynein): 50% of them have a mirror-reversal of all internal organs, relative to normal humans [11].

The mystery is why a chiral bias is needed at all, in the symmetry broken cases. A mirror-reversed individual is just as viable, and interactions between individuals only occasionally depend on their having the same handedness. Statistical physics can illuminate one plausible evolutionary motive for the chiral bias. Whenever L/R asymmetry is developed after an embryo is extended and multicellular, spontaneous symmetry breaking cannot happen instantaneously but must evolve over some time, during which larger and larger parts of the system “agree” as to the final sign. This is analogous in statistical mechanics to *quenching* from a high-temperature disordered phase, into an ordered state. In the absence of a bias field, overly rapid quenching leads to a mixture of several domains: in some of these the symmetry gets broken one way, in others it gets broken the opposite way. In an animal embryo, that would produce a spatial mishmash of normal and inverted regions, called “heterotaxia” in medicine, and responsible for serious congenital defects such as the duplication or absence of organs. By using a symmetry-breaking field, the embryo can afford to “quench” more rapidly – time is often at a premium in development – yet not risk heterotaxia.

The above reasoning applies most strongly for phyla in which the fate of cells is fixed late in development, by some form of patterning. In examples where the style of development is to fix fates early – even in the first three divisions – this concern appears less critical. That suggests one possible reason why molluscs (an early developing phylum) have repeatedly speciated with a flip of the chirality, and why the nematode *C. elegans* may tolerate a high incidence of reversed individuals (Ref. [27], p. 3505).

The “symmetry breaking” notion has been discovered independently in the context of development without help from statistical mechanics. In particular, this may be the most important notion in Brown and Wolpert’s ground-breaking paper [1]. Also, Wood’s “choice execution” (Ref. [2], p. 76) is approximately the same notion as spontaneous symmetry breaking.

2 Cell division and actomyosin layers

Animal cells lack rigid cell walls, and hence can realize handedness (like other kinds of organization) using motility, changes in shape, or displacements with respect to adjacent cells. The actin component of the cytoskeleton exerts forces in two ways:

- (i) Bundles of myosin molecular motors form bridges between actin filaments, walking along them and thus causing relative motions of the filaments. The actin and myosin combined constitute an active medium (called actomyosin)
- (ii) Actin polymerization generates an average tip force via the “Brownian ratchet” mechanism [28]. Such forces extend the pseudopods (projections of the cell body) that enable the (crawling) motility of eukaryotic cells.

This section takes up the first (actomyosin) story; I will return to the second (polymerization) kind of mechanism in Sec. 4.2, speculatively.

In this section, I lay out for the first time a comprehensive picture of actomyosin handedness at three levels, starting with the intercellular level where I first summarize the observations of spiral cleavage in snail embryos (Sec. 2.1) – *C. elegans* embryos are roughly similar – and then show they follow if cell division is associated with a particular twist (Sec. 2.2). The next level is a two-dimensional continuum theory for the actomyosin layer in one cell (Sec. 2.3), where I point out that the aforementioned twist and two other striking chiral behaviors are all consistent with the *same* handedness of the continuum model; lastly I present a microscopic-level screw-mechanism scenario, depending on the myosin stepping motion along an actin fiber (Sec. 2.4), which predicts the correct handedness at the continuum level.

2.1 Introduction

The initiation of left/right asymmetry has been studied carefully in two kinds of invertebrate, which have a pattern of development such that a cell’s fate (i.e. what kind of cell its descendants become) is determined at the few-cell stage: molluscs (specifically snails) and *C. elegans*. In both cases the mechanism involves “actomyosin”, the layer of actin filaments and myosin motors immediately under the cell membrane. I conjecture that the “collective level” mechanism is a twist about the division axis during each cell division.

First I review some facts. In snails [29] (specifically *Lymnaea stagnalis*), after the first two divisions along mutually perpendicular axes, an embryo consists of four cells in a (nearly) perfect square. These divide vertically, producing four (smaller) daughter cells. As is very long known, the square of

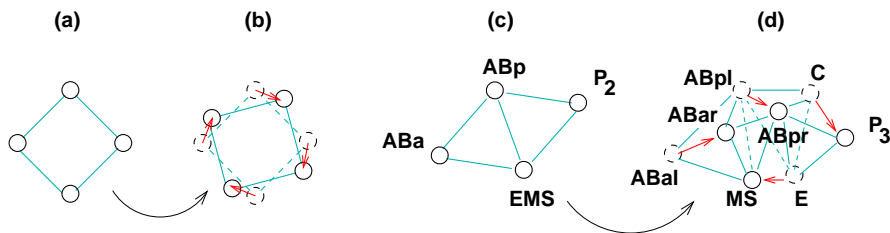


Fig. 1 Breaking L/R symmetry at the four-cell stage through division with a twist (a,b) The 4-cell and 8-cell stages in the snail embryo. Cell centers are represented schematically by circles, and connected by lines if they adjoin (lower layer is dashed). Arrows connect cells that divided. From the nearly square embryo in (a), the four daughter cells are displaced around the 4-fold axis to the intercell furrows as in (b), the “spiral cleavage.” (c,d) 4-cell and 8-cell stages in the asymmetric *C. elegans* embryo; the displacement of dividing cells can be explained by a twist of the same sense as in the snail. Dorsal/ventral ($+z/-z$) and anterior/posterior ($+x/-x$) axes are shown; the $+y$ axis (right side) is out of the page.

daughter cells breaks the symmetry by rotating $\sim 45^\circ$ *clockwise* (as you look down on the square) so as to sit in the crevices between the original cells, the so-called “spiral cleavage” This is shown schematically in Figure 1(a,b). Which way this rotation goes decides the handedness of the final snail, as proven by micromanipulation experiments in which the daughter cells were pushed the other way [30]. It was earlier shown that a mutant which has the opposite twist at the 8-cell stage also ends up with an oppositely twisted shell [29].

In *C. elegans* embryos, the embryo with four cells is also planar but unsymmetric. The next cycle of divisions (to eight cells) makes it three-dimensional. A cartoon of this process is shown in Fig. 1, which compares molluscs and *C. Elegans*. It can be seen that the screw sense of the motions is the same as in the snail spiral cleavage, as first perceived by Wood [2,4]. The handedness of the final embryo is determined by these divisions, specifically at the six-cell stage as shown long ago by Wood using micromanipulations [2, 4, 19, 20]. More recently Ref. [31] has carefully studied all chiral asymmetries in the early divisions of *C. elegans*, including cell protrusions and adhesion.

Right after the symmetry-breaking division at the four-cell stage, some chemical signal must be passed between the cells, depending on which cells are neighbors. Since the neighbor relation has become asymmetric, this tells the cells which is L and which is R; that “bit” of information is preserved in subsequent divisions for the descendants of these cells, and is expressed functionally at a much later stage. The early-stage signal has been identified in the *C. elegans* case [20].

Experimentally in snails, the twist depends on actin (it is disrupted by the depolymerization agent latrunculin) but *not* on the microtubules [29] that (e.g.) constitute the mitotic spindle. Incidentally, mutants that will have the wrong handedness initially stay *symmetric* at the \rightarrow 8 cell division, but a *distinct* chiral mechanism (also involving actin) comes into play immediately afterwards; I will propose an explanation in Sec. 2.2.3.

2.2 Intercellular level story for snails: twisted cell division

I start by addressing the “intercellular” level mechanism. It is already known that the left/right asymmetry in snails is actin/myosin driven [29].

2.2.1 Facts of cell division in snail embryo

Let us walk through the stages of the division with spiral cleavage. Figure 2(a,b,c) show a cartoon of the divisions in the wild-type snail embryo. We are looking down from the animal (+ z) axis. The first division is into cells called AB and CD. After the second division [Fig. 2(b)] the cells almost form a planar square.

The third division axis is normal to the (approximate) plane of the four cells, and produces four smaller daughter cells on the + z side. The defining event of “spiral cleavage” is that the daughter cells rotate, clockwise (looking down the z axis) in the “dextral” form, so as to lie in the furrows between the parent cells. In the wild-type dextral, the spindle axis of the third division is observed to be already tilted *before* that division (so called “spiral deformation” [29]).

The “sinistral” mutant is outlined in Fig. 2((d,e,f). In this case, there is no spiral deformation: the daughter cells only rotate later on, during furrow ingression (i.e. the time they get pinched off from the mother cells) – and they turn counter-clockwise (CCW), opposite to the wild type.

2.2.2 Wild-type snail: latent-spindle mechanism

The observed (handed) positioning of the cells is compactly explained if we posit that two dividing cells acquire a relative twist, always of the same screw sense – let’s say *clockwise*, as you view one cell from its neighbor. This “division twist” must be driven by flows of the actomyosin layer associated with the cell membrane, which (in particular) concentrates along the dividing plane and forms the contractile ring that pinches off the daughter cells. (The large-scale, chiral flow will be addressed in Subsec. 2.3 at the single-cell continuum theory level.) Then, spiral cleavage can follow as a purely mechanical consequence. But I find *two* alternative mechanisms, derived from the *same* mechanics posited above but acting at *different* times relative to the division, that produce rotations of the four daughter with *opposite* senses. Both mechanisms are illustrated in Fig. 2.

We can call the first mechanism the “latent spindle.” The key assumption specific to this mechanism is that, even before one division is complete, the mitotic axis to be used for the *next* division (along a perpendicular axis) exists, in some latent form. The physical determinants of this might be centrioles (molecular complexes in the cell which, when present, anchor the spindle’s endpoints); being attached to membrane, they will get carried along by the large-scale actomyosin/membrane flow. Indeed Wood (Ref. [2], pp. 74-75) specifically suggested centriole positioning as an ingredient of the mechanism

for snails, though in a different way than I proposed. (He suggested distinctive segregation of the inherited and the newly formed spindle poles that are at either end of the division axis.)

Initially, the latent axes are parallel in the two cells; but the latent axes get carried along by the division twist of the prior division as it proceeds, so they get tilted relative to each other. Then, as figure 2(b) shows, the combined twists from the first two divisions imply spindle alignments for the third division that are predicted to be tilted around the fourfold axis exactly as seen experimentally in the four-cell stage, called the “spiral deformation” [29]. When the daughter cells subsequently divide along these tilted axes, they are biased with a *clockwise* rotations relative to the mothers, as seen experimentally in wild type [Fig. 2(c)].

2.2.3 Mutant snail: adhesion-constraint mechanism

The second mechanism might be called “adhesion constraint.” It means a tendency to twist about each division axis that is frustrated by the constraints of adhering neighbors, but drives twist by larger groups of adhering cells. Start again with the square of cells resulting from the first two divisions; imagine that the four daughter cells, before separating from the four large mother cells, formed adhesions with each other. What does the *same* postulate predicts for the dynamics *after* (or while) the small daughter cells divide?

If we had isolated mother/daughter pairs, torques due to the cortical flows would drive each daughter cell to rotate *counter-clockwise* around the division axis (looking down the z axis), as shown by the arrows in Figure 2(e). But after the four daughter cells form adhesions, they are no longer free to rotate separately, but only as a rigid assembly. The net torque on this combination turns the square of four daughter cells counterclockwise, i.e. *rightwards* as seen from the mother cells, which is *opposite* to the sense of rotation of the latent-spindle mechanism of Sec. 2.2.2.

Thus, the *same* mechanism produces *contrary* effects, depending on the time in the division process at which it acts. This suggests the hypothesis that, in the snail *L. stagnalis*, both kinds of handedness can be explained by a single chiral mechanism – the difference is ascribed to a non-chiral property; namely, it appears that the spindle-orientation effect is the stronger effect in the (sinistral) wild type, but is missing in the (dextral) mutant, so that the secondary division effect takes over.

2.2.4 Tests of division-twist idea?

An immediate consequence of the idea is visible already at the four-cell stage. If the first divisions have the *same* sense of twist as needed to predict the spiral cleavage, the embryo should be slightly warped, with the A and C cells raised (so they touch on the $+z$ side) and the B and D cells lowered (so they touch on the $-z$ side), as illustrated in Fig. 2 (b). This agrees with the sense of warping observed experimentally (Ref. [29], figure 2B).

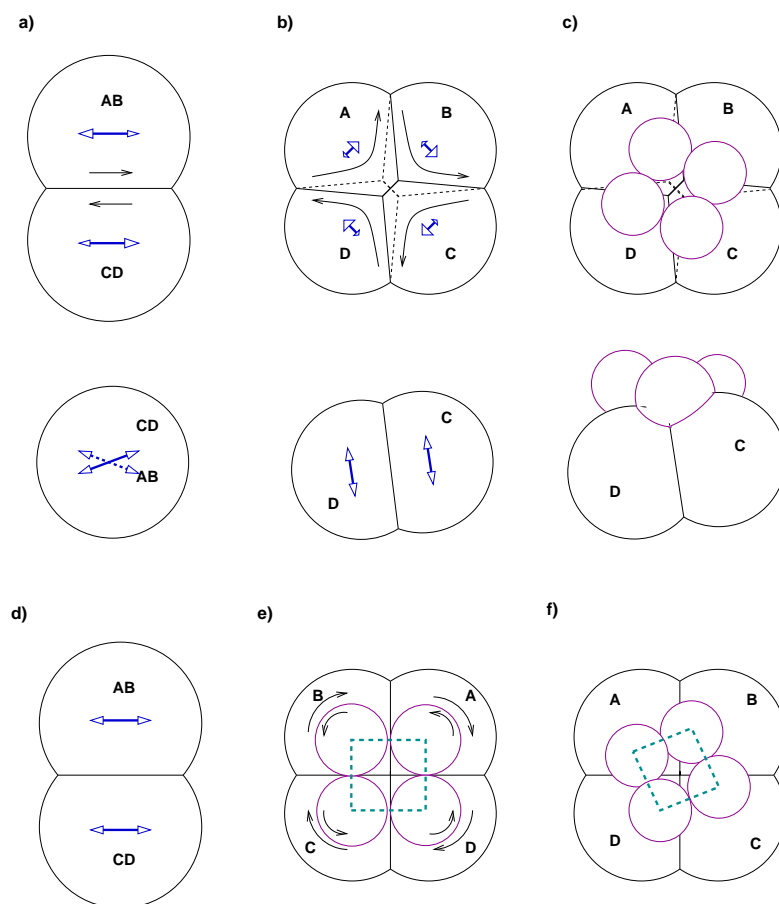


Fig. 2 (a)–(c) Early divisions in wild type (sinistral) snail, two views of each (left: down z axis, i.e. from the “animal” direction; right, down x axis). Thin arrows show the predicted large-scale cortical flow; heavy arrows show a latent (incipient) spindle direction. (a). two-cell stage (named AB and CD) (b). four-cell stage; the next axis is almost normal to the plane of the cells (c). eight-cell stage. Parts (d)–(f) are a cartoon of divisions in the dextral mutant snail (d) The latent spindle directions are not twisted in the first division (nor in later ones) (e) After the four daughter cells bud off, the actomyosin layer flows as indicated by the arrows. Since the four daughter cells are already connected by cell adhesions (symbolized by dashed square) the combined effect of the flows is for them to rotate as a rigid body, in the sense shown in (f). Note that, relative to the cell boundaries, the actomyosin flow has the *same* sense in (b) and in (e), but this leads to *opposite* outcomes in (c) and in (f), depending on whether that flow is active before or after division.

On the other hand, the mutant sinistral *L. stagnalis* should lack the main warping; indeed, according to the adhesion-constraint scenario, in the second division-cells B and C should twist as a unit after they separate from cells A and D so the warping should occur in the reversed direction. Indeed, figure 2B of Ref. [29] shows an absent or perhaps slightly reversed warping in the mutant.

Of course, the last observation only shows that the twist occurs in different cell divisions. To test my proposal that the *same twist sense* acting at different times can produce the observed effects, one apparently needs mutations or drugs that change the duration of the respective stages, or that change the strength of cell-cell adhesion governing the adhesion-constraint mechanism. A mechanical test might be to remove three of the four daughter cells from the mutant, in which case the remaining cell (freed from constraint) ought to rotate around the axis joining it to the parent cell.

2.3 Micro story: continuum equations

I suggested in the last subsection that the ultimate handedness both snails and *C. elegans* would be explained if the actomyosin layer, around the division furrow where it concentrates, shears in a *clockwise* (CW) sense, as you look down at the membrane, as marked by the small arrows in Fig. 2 and by the straight arrows in Fig. 3(c). motion in the actomyosin layer, around the time of cell division, can drive a twist between the two dividing cells. In fact we can see two other striking chiral phenomena *with the same clockwise sense* in actomyosin cortical layers (subsec. 2.3.1); this would be explained if pairs of the units forming the layer interacted with a clockwise twist, which can be represented at the collective level by a single “skew stress” parameter (subsec. 2.3).

2.3.1 Chiral phenomena in actomyosin layers

Animal cells typically have a cortical (adjacent to membrane) actin-myosin layer. This practically two-dimensional medium is responsible (in some theories) for the effective surface tension of cells [32]. In the form of the “contractile ring” [33,34,35,36], an array of roughly parallel filaments that contract to pinch off the two cells from each other. Note the myosin in these layers is a form of myosin II, the same myosin found in muscles, which is a non-processive motor protein (does not stay on the actin for many steps).

Massively chiral behavior is already known in the actomyosin layer in two instances, both in egg cells (convenient for imaging since they are so much larger than regular cells).

- (1) The *C. elegans* egg, before its first division, develops a polarity which includes a segregation of the actomyosin layer towards the anterior end, shown by a denser shading in Fig. 3(a). Towards the end of that process, all the actomyosin rotates around the anterior-posterior axis [37], in the *clockwise* sense, as one faces the anterior end from outside the cell. (This phenomenon is familiar to *C. elegans* researchers and visible in movies, but has not been commented on in print to my knowledge.)
- (2) Danilchik *et al* [38]. treated *Xenopus* (frog) eggs with a poison (butanedione monoxime = BDM) that partially disrupts the actin network. When the contractile ring begins to form along an egg’s future cleavage plane, it develops an array of parallel actin bundles shearing each relative to the next, such that the local vorticity is *clockwise*, as abstracted in Fig. 3(b).

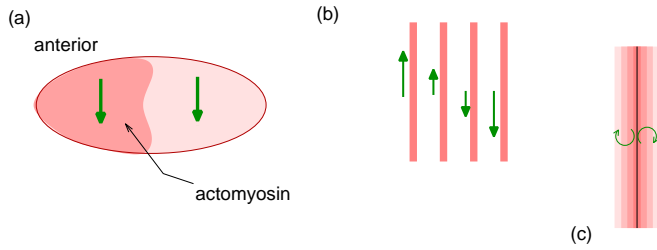


Fig. 3 Observed chiral phenomena in actomyosin layers. (a) Egg cell of *C. elegans* at end of the polarization in which actin (shading [pink online]) concentrates towards the anterior end. Just before the division furrow forms, a concerted motion is seen as indicated by the large arrows. (b) Schematic of the *Xenopus* egg, in which bundles of actin (stripes) around the incipient contractile ring were observed in Ref. [38] to shear with relative velocities as shown by the arrows. (c) A band of actin is shown with densities represented by shading [pink online]. The continuum theory of Sec. 2.3) with $q > 0$, or equivalently a clockwise interaction of pairs (small arrowed arcs), gives no net force in a uniform distribution of actin, or at the density maximum in the middle, but tends to drive a clockwise shear on either side, in accord with the motions assumed in Figure 2.

This mechanism does *not* depend on actin polymerization (as checked by the null effect of latrunculin, which inhibits polymerization).

- (3) Finally, of course, there are the early divisions in snails and in *C. elegans*, both implicating actin as detailed in Sec. 2.1; as illustrated in Fig. 2, this also entails a clockwise shear around the division furrow, as cartooned in Fig. 3(c).

2.3.2 Form of continuum equations

Our philosophy is to seek the simplest set of continuum equations that are compatible with symmetry and Newton’s law of action/reaction, and that have a chiral term. (Note that our layer is in contact with the membrane above and the cell fluid below, which exert forces such as viscous damping, so our equations need not be invariant under boosts.)

The necessary ingredient is that the “units” constituting our medium have a pairwise interaction that tends to rotate them in a fixed sense (say clockwise) about the midpoint between them. Naively, one might expect this to drive the velocity field to have a vorticity, $\partial v_y / \partial v_x - \partial v_x / \partial v_y < 0$. However, so long as the density is uniform, the mean force on a given “particle” is zero by symmetry, since it has (on average) equally many nearby particles on either side. Therefore, chiral forces are associated with *gradients* in the actomyosin density.

I believe the simplest functional form for the continuum theory of a two-dimensional actomyosin layer is that the stress tensor $\sigma(\mathbf{r})$ acquires the form

$$\underline{\sigma}(\mathbf{r}) \equiv \begin{pmatrix} \sigma_{xx} & \sigma_{xy} \\ \sigma_{yx} & \sigma_{yy} \end{pmatrix} = \begin{pmatrix} p & q \\ -q & p \end{pmatrix} + \underline{\sigma}_{drag}(\mathbf{r}) \quad (3)$$

where p is the (two-dimensional) pressure, q is an unusual “skew stress” ($q > 0$ for the CW interaction that I posited); $\underline{\sigma}_{drag}$ is the contribution of drag to the stress tensor. Both $p(\mathbf{r})$ and $q(\mathbf{r})$ should be functions of the local number density $\rho(\mathbf{r})$ (and any other collective state variables) according to some constitutive equation. To *rigorously* define q (or even p), one would need for the actomyosin to form a statistically uniform and stationary steady state.

It is a general dictum in mechanics that $\underline{\sigma}$ should be a symmetric tensor, but that is not logically necessary when torques can be applied in the bulk interior, as in many actively driven systems. In the case considered by Ref. [39], the torque is due to rotations by each particle around its center of mass; in our case, it comes from the interaction of two particles coupled to a membrane and cell fluid that define a preferred frame. Specifically, the component σ_{yx} (e.g.) is defined as the y component of force being exerted on the $x < 0$ side of a plane normal to the x direction. Clearly, whenever a unit-unit interaction crosses that plane, it contributes a force in the $+y$ direction, meaning $\sigma_{yx} = -q < 0$, similarly $\sigma_{yx} = +q > 0$.

Often these systems have another state variable besides the density, namely the bidirectional (or “nematic” in statistical physics) orientational alignment of filaments. In that case, the stress tensor has an additional traceless symmetric term with its axes aligned with the nematic axes. Furthermore, in our chiral systems the stress axes will generically get rotated a bit from the nematic axes (in a definite sense). I will not consider this complication in the present paper.

The consequence of (3) is that the local force density (per unit area) is

$$\mathbf{F}(\mathbf{r}) = \nabla p + \hat{\mathbf{z}} \times \nabla q - \lambda \mathbf{v} + \mu \nabla^2 \mathbf{v} \quad (4)$$

where $\hat{\mathbf{z}}$ is the unit normal to the layer. The last two terms are, respectively, drag due to the membrane, and drag due to shear of the actomyosin layer. The first drag term models the viscous damping as the actomyosin slides past the (fixed) membrane and the bulk fluid (cytosol) of the cell which is entrained by the cytoskeleton that permeates it. Inertia is negligible at our low Reynolds numbers so the velocity field $\mathbf{v}(\mathbf{r})$ is the solution of $\mathbf{F}(\mathbf{r}) = 0$,

2.3.3 Dresden three-dimensional continuum equations

The MPIPES (Dresden) group [39, 40] have been developing a comprehensive three-dimensional continuum description of active, chiral media, which is less ad-hoc than the one presented here, but also more complicated.

The key differences are that

- (i) They model a *three* dimensional actomyosin fluid. Presumably an effective two-dimensional model can be derived from it, so as to model the (relatively thick) cortical actomyosin layer by a density that falls off with distance from the membrane.
- (ii) Their model takes into account not only the angular momentum inherent in the velocity field, but separately the angular momentum due to internal rotations of the microscopic rigid units constituting the active fluid. This

seems motivated by the case that the active entities are swimmers. In a sufficiently damped limit, as in the case of the actomyosin surface layer, one can eliminate this kind of orientational degree of freedom and obtain an effective model in which angular momentum injected by the active degrees of freedom is attributed directly to the center-of-mass degrees of freedom.

Overall, their philosophy is to incorporate all possible terms allowed by symmetry, which means quite a few unknown coefficients. Here, in contrast, I tried to adopt the *minimal* model that is internally consistent and appropriate to our particular system.

2.3.4 Applying the equations

The motivation for this continuum theory was the cell division story of Sec. 2.2. What does the second term in (4) say about dividing cells? The contractile ring and furrow, along a dividing cell contact line (as seen in Fig 2), is a local maximum of the actomyosin density. In light of the density gradient in either direction away from the line, the chiral dynamics of (4) imply a clockwise shear adjacent to these boundaries; the arrows shown in Fig. 2 correspond to $q < 0$ in (4), as shown in Fig. 3(c).

The same equations could be applied to a different example of emergent chirality in which the elementary units are cells rather than actin fragments, and the pair interactions are due to actin-driven cell motility and/or cell-cell adhesion, rather than to myosin bridges. This is applied in Sec. 4.3 to spontaneous chiral flows in a population of eukaryote cells.

The anterior/posterior polarization in the *C. elegans* egg can be represented by an externally imposed gradient in the actomyosin activity rates, analogous to the enhanced activity postulated in a band which triggers formation of the contractile ring [36]. The rather uniform rotation of the entire actomyosin layer does not follow easily from the Eq. (4), which describes a flat layer and assumes the total *force* in that layer is zero. But we fit this into the same framework if we step back from the continuum theory to the underlying idea of a density-dependent clockwise torque. The anterior end contributes a net torque around the long axis in the CW sense (as seen from that end), while the posterior end contributes with the opposite sense; but the anterior term is much larger (as the layer is denser there). Thus if all parts of the actomyosin layer are rigidly linked, the whole layer rotates in the sense of the combined torque, which is CW as observed.

In principle, many experimental tests are possible using video data of the actomyosin layer as already used in Ref. [41]. Eq. (4) implies visible local velocities transverse to any variations in the density, whether they be random statistical fluctuations, or cuts in the cortical layer made by laser ablation [41].

2.4 Actomyosin: molecular level story

What microscopic mechanism can implement the chiral inter-unit force? By the fundamental symmetry notion invoked in Sec. 1.3, any such mechanism

must involve the membrane. (In its absence, the system has a symmetry of swapping the up and down directions by a 180° rotation, but the handedness would be opposite when viewed from the down side.)

I will develop an explanation of the “screw” class (in the categories of Sec. 1.4), i.e. depending on the actin fiber itself being a helix, and using myosin II (the kind in the actomyosin layer as well as in muscle cells). To start, note that in a standard motor protein assay, in which actin filaments glide on a surface coated with myosin II, actin is found to twirl CW looking towards the plus end [42]. (CCW in the direction of filament motion; it has not been explained why an opposite sense was reported in the past [43].) This indicates a CCW azimuthal component of myosin II’s step (as it moves towards the plus end).

The detailed theoretical explanation [44] shows that the rotation depends on a commensurability of the myosin step with the lattice of binding sites on actin (considered as a two-dimensional lattice wrapped around a cylinder). Thus the handedness of the typical step could alternate in sign as the myosin length is monotonically reduced (as is engineered in some experiments).

2.4.1 Details of myosin up/down mechanism

The dynamics of actomyosin depend on myosin bridges that connect two actin filaments, with multiple myosin heads at either end [47]. Due to the multiple heads, the bridge’s motion along the filaments might effectively be processive, even though individual myosin II molecules are not processive. (Previously, the processive myosin V had been observed to spiral as it traveled along an actin filament [45].) This partially justifies our drawing the myosin as if it stayed processively on the actin, but that picture is only for convenience: if the myosin only gives one power stroke before releasing, it will still drive a net twisting of the actin if that stroke has the azimuthal component.

In contrast to (say) the thin plant cell microtubule layer of Sec. 3, the actin cortical layer in animal cells is 100 or even 1000 nm thick [46]. This contains many actin fibers extending transverse to the membrane (from which they nucleate and grow in various directions into the cell fluid). This offers an opportunity to relate the handed motion of the myosin II around a filament, to the handed motion orbiting that we posited in subsec. 2.3.2 between two of the units (namely two actin filaments). Note that the actin nucleates on the membrane via formins which are associated with the plus end, so actin filaments are polarized *towards* the membrane (“upwards”).

Consider two parallel actin filaments, both polarized upwards, and connected by a myosin bridge, as shown in Figure 4 (a,b). Each myosin head (or multi-head) walks upwards, tending to spiral CW around the actin (as viewed from above the membrane, opposite to their direction of motion). However each is constrained by the bridge connecting it to the myosin head on the other filament. This produces a net torque which tends to rotate the pair CW around the middle of the bridge, the very clockwise force we had posited.

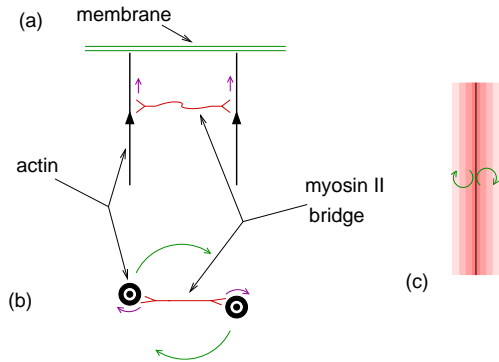


Fig. 4 Handed forces due to azimuthal motion of myosin II (a). Side view of two actin filaments, polarized upwards as marked by large arrowheads on the filaments, and connected by a myosin bridge which walks upwards as marked by small arrows [purple online]. Only one myosin is shown at either end of the bridge; actually there are many. (b). Top view (from outside membrane) of the same filaments. As the myosin II motors step towards us, the screw component of their motion is in the direction shown by the small arrows [purple online]. This tends to “roll” each filament CCW, which in turn “rolls” against the fluid to drive the pair in a clockwise motion (large arrow arc [green online]). (c). same as Figure 3(c). A band of actin is shown with densities represented by shading [pink online]. The clockwise relative interaction of pairs (arrow arcs [green online]), gives a cancelling mean force at a symmetry center such as the band’s center. But in the band’s wings where the density is different on either side, there is a net force which follows a clockwise pattern on a larger scale.

2.4.2 Questions about this theory, and experimental tests

It is not easy to graft this handedness notion onto a quantitative model of the actomyosin layer, for no such model exists: too few of the parameters have been measured experimentally in actomyosin. The existing models for actin contractility [48,49] are qualitative at heart.

The microscopic screw-mechanism hypothesis, presented here, implies a universal sense of handedness due to the intrinsic properties of actin and myosin II. If we take this seriously, it makes a powerful prediction: reversed handedness is possible, but its mechanism can *never* be functionally equivalent to the wild-type’s at the bottom level. There is one qualification: as handedness is propagated from its original cause, either from lower to higher levels in these mechanisms of the origin, or from upstream to downstream in the signaling cascades that specify every cell’s fate in development, the response in the reversed organism probably does become functionally symmetry-reversed at some point. In snails, though, the external shell shape is subtly different between the mutants and wild type [50]; of course, this may be one of the many independent effects expected from a mutation affecting the cytoskeleton.

At first glance this sweeping prediction seems to be perfectly confirmed in the qualitative difference between dextral and sinistral mutant snails observed in Ref. [29], as summarized in Sec. 2.2.3. the dextral snails. However, a further observation seems to contradict it. Namely, snails that are sinistral *as*

a species show a spindle-orientation effect (spiral deformation) in the opposite sense. [29]. Furthermore, the difference in external shell shape between wild-type and mutants also gets flipped in those species [50]. We expect the chiral sense of the large-scale flow to depend on universal properties of non-muscle myosin II, and hence not to flip its sign from species to species. If further observation really confirms that the sinistral species are perfect mirror images, we might be forced to abandon the screw mechanism for the “anchoring” type mechanism (in the classification of Sec. 1.4). The respective anchoring molecules would not be mirror-images of each other; all that is necessary is that they would bind myosin molecules with the heads oriented in opposite directions.

Of course, to flesh out the physical picture presented above, it ought to be extended at least to give an (order-of-magnitude) estimate of the expected twist rates. This is not hopeless: using hydrodynamics we can certainly estimate the chiral component of the force between two vertical filaments from known parameters of the motors. The main unknown is the number of such myosin bridges, which – conceivably – might be related to the contractile force within the layer as measured in laser ablation experiments [41]).

3 Plants and 2D microtubule array

The origin of handedness in plants involves another dynamic, cortical fiber array – not of actomyosin as in animal cells (Sec. 2) but of microtubules (mt) [51]. A major difference is that whereas few physical parameters are known for the actomyosin array, they are all quantitatively measured for the plant cell microtubule arrays. The microtubule array is a template for the cellulose fibers formed outside the membrane, which forms the cell walls characteristic of being a plant.

3.1 Macroscopic root behavior

On the large scale, many species exhibit systematic handedness in their roots, shoots, or flower shapes:

- (1) The growing root’s tip tends to trace out a helix with a consistent sense (flagrantly so in climbing vines).
- (2) Roots growing against a tilted hard surface have a handed bias (in that plane) from the most directly downward direction, called “root skewing” [52].
- (3) The “cell files” – longitudinal rows of cells on the outside of the root – twist around the root’s axis.
- (4) The cells (long cylinders aligned with the root’s macroscopic axis) have membrane-associated arrays of parallel microtubules which *spiral* around the cell in a characteristic sense.

In the model species *arabidopsis*, mutations that reverse the sign of one behavior also reverse the others [52, 53], suggesting that the microtubule array

is the microscopic origin. Indeed, mutants with strongly helical behaviors turned out to be mutants of the tubulin molecule itself [53].

Can the macroscopic behavior, at least, be explained from mechanics and simple biological models of the root growth? Recent experiments have elucidated root twist by three-dimensional imaging of *Medicago Truncatula* roots, growing downwards in clear gel. The cell files are untwisted until the tip encounters a resisting layer, upon which they become helical (and the root's buckling develops in a helical form) with a reproducible bias in handedness [54].

Thus, it appears the twist is an active response to sensing of a *longitudinal* force by the tip, an unusual example of the touch responses known as “thigmotropisms”; the roots also have an active response to gravity called “gravitropism”. These tropisms usually are not chiral; they involve a transverse bending of the root in a direction aligned with the transverse force, or the component of gravity as sensed by the tip; it is transmitted somehow by the hormone auxin to the region a short distance back from the tip where new cells are elongating, which implement the bending by elongating more on one side than the other. The observed phenomenon of sinusoidal-like alternate bends (“root waving”) can be understood in such a scenario [55].

The intermediate organism-level step, how the microtubule array's handedness implies the macroscopic chiral thigmotropism, is still unclear. Hashimoto [56] has suggested a passive mechanical explanation: the inner layers elongate deficiently (the strongly biased mutants tend to have defects in the microtubule array leading to loss of cylindrical cell shape), while the epithelium elongates more, which in turn triggers a helical buckling of the latter. However, this picture in itself is a spontaneous symmetry breaking: some small biasing is still needed to give it a regular handedness.

It can be noted here that an early mechanics paper related the macroscopic helical growth of the fungus *Phycomeces* to the spiral arrangement of the chitin fibers forming its cell walls, analogous to the cellulose fibers in plant cell walls [57]. The cytoskeleton in fungi is much less thoroughly studied than in animals or plants; since they are more closely related to animals than plants, one could speculate that an actin cortical layer takes over the role of the microtubule array in plant cells.

3.2 Cell level mechanism: microtubule arrays

I turn to the cell level mechanism. Video microscopy shows that microtubule arrays get oriented in a collective process governed by the following rules: [58, 59]

- (1a) *Growth*: The + end of the mt grows quickly, while the – end steadily depolymerizes, more slowly than the + end grows.
- (1b) *Spontaneous catastrophe*: the + end can spontaneously transition into a rapidly *depolymerizing* state, so that the whole microtubule may soon be undone: this is called a “catastrophe”. There is also a rate for transitions back to the growing state.

-
- (2a) *Collision and entrainment*: When a growing mt hits another at a relative angle less than $\sim 40^\circ$, it bends and *entrains* parallel; this process generates bundles..
 - (2b) *Collision-induced “catastrophe”*: If the angle is larger, the growing mt suffers a “catastrophe”
 - (3a,b) *Nucleation and branching* New mt’s nucleate both (a) at random places and (b) on existing mt’s; the latter have branching angles centered around $\sim 40^\circ$ or so from the + direction [62], but also a significant number are at angle 0, i.e. are born entrained [62].

The rates for these processes have been measured experimentally [58,60,61,62] and used recently in numerous mathematical models [63,64,65,66,67,68,69] which have been reviewed in Ref. [70]. It still unsettled [70] whether the parameters in Rule (i) put the single-mt behavior just above or just below the threshold at which it would grow without bound; this question is not critical in the array state, where mt growth is actually limited by collisions [Rule (iii)]. Processes (ii) and (iii) both tend to drive the mt’s into a steady state in which microtubules tend to be parallel or antiparallel to some direction in the plane which is (so far) arbitrary; such a bidirectional, symmetry-broken phase is labeled “nematic” in statistical mechanics. (Experimental arrays actually seem to be polarized in *one* direction, not bidirectional [73], but this point is unimportant for the chiral properties.)

A less clear aspect of the array alignment story is, why does the observed array orientation have a systematic relation – mostly transverse, but tilted chirally– to the cell’s long axis? The widely accepted explanation for this is the cell caps [72], a sort of finite size effect. One can treat the cell’s entire membrane as roughly a flat rectangle having periodic boundary conditions in the azimuthal direction, but open boundary conditions the other way, representing the cell’s end caps. These boundaries orient the microtubules. The long-range collective orientational ordering of the array then propagates this information over the entire surface.

I would propose an alternative variant of the boundary-conditions explanation of orientation bias; my version depends on the azimuthal periodicity but not on the end caps. We know, from simulations or common sense, that before the system coarsens into a single ordered domain, the orientational correlations extend much farther in the direction parallel to the microtubule orientation than transverse to it. When that orientation happens to be azimuthal. the correlated domain has its best chance of growing all the way around the cell and finding itself, thereby locking the orientation. (This presumes the cell’s circumference is smaller than its length.) Finally, yet another possible explanation of the transverse orientation bias is that the microtubules independently sense the curvature direction of the membrane (see Sec. 3.5).

The least clear aspect of array alignment is why that orientation *deviates* from transverse with a definite handedness, on average, as observed experimentally. Let’s start with a coarse-grained description at the level of a continuum theory or a mean-field theory. Imagine the array’s collective order parameter angle $\alpha(t)$ *precesses* at some average rate [6],

$$d\alpha/dt = \omega_0. \tag{5}$$

In fact, video imaging showed local rotations of array domains in elongating plant cells [73] and Wasteneys also speculated there could be a global precession rate [74]. A dynamic rotation is also suggested by morphologies of some plant cells that have multiple layers of cellulose fibers, each rotated relative to the one underneath [75].

Meanwhile, whatever its origin, the transverse orientation bias will appear as a competing term added into (5). Then the combination of the precession force and the transverse bias yields a final orientation deviating in a particular sense from transverse, by an angle α_0 dependent on the relative strength of the two factors [6].

3.2.1 Realizing chiral bias in microtubule simulations?

Let us now step down in level and consider explicitly the stochastic dynamics of many microtubules that follow the above listed event rules. Chiral bias can be incorporated in the dynamics via either kind of event that is an interaction:

- *Branching*: the branching angle distribution, of a new microtubule relative to the old one, is asymmetric between left and right.
- *Collision*: the outcome of an mt-mt collision depends on which side the growing mt is impinging from [Rule (iv)].

Since the constituents are chiral, it is a trivial observation that no exact symmetry dictates that either process has an exact L/R symmetry. Then a nonzero precession rate is *generically* expected; however, it might be imperceptibly small in practice, and will be suppressed once orientational long range order extends all the way around the cell.

The only simulation that has produced a helical bias is [68]; that was accomplished by combining a chiral bias in the branching rates with an ad-hoc simulation condition, in which the rules were changed partway through the run. This change probably realized the competition with a transverse orientation bias as I suggested just above, with that bias effectively being provided by open boundary conditions representing the cell caps in this simulation. Subsequently, Ref. [69] (their Sec. 3.4) also simulated the effects of chiral branching bias under various conditions, and observed precession but did not quantify it; they concluded its effects are too weak to account for the reorientations seen in Ref. [73]. It remains to be checked whether a collision bias can have a stronger effect [71].

3.3 Molecular level: mechanisms for precession?

Let us step down again to the molecular level: here we have stronger reasons to predict precession of the array based on either of the possible aligning mechanisms, as a handed bias of the branching is *observed*, and a bias of the collisions can be argued theoretically.

3.3.1 Branching mechanism

A subtlety of the experimental data is that although Ref. [62] (page 2300) reported an equal likelihood of positive and negative branching angles θ_b , they also reported a statistically significant difference in the *distribution* of angles. Just as the effectiveness of branching for aligning the array is roughly $\cos 2\theta_b$ as derived from a mean-field theory [64,69], so the effectiveness for precession should be $\sin 2\theta_b$. This quantity was estimated based on the histograms in Ref. [62], figures 2C and 3E, and indicates a significant bias [71]. The sign is $\sin 2\theta_b > 0$, indicating a tendency to precess CCW, that is $\omega_0 > 0$ in (5).

It is expected that one of the “membrane associated proteins” (MAP) mediates the branching, by binding to the existing mt and nucleating the new one. Since the mt consists of ~ 13 equivalent protofilaments, the MAP could in principle bind at any azimuthal angle around the mt; presumably this orientation determines the direction in which the nucleated mt emerges. The observed left/right differences in branching mean that the nearby membrane conditions the nucleated mt’s direction; presuming the latter is determined by the MAP orientation, it means that is constrained by the membrane. This is an example of the fundamental symmetry considerations of Sec. 1.3; it may be rather obvious, but it logically leads to an interesting biological prediction: there must exist some physical interaction between the MAP and the membrane – an interaction which has not yet been identified experimentally. By “physical interaction” I do not necessarily mean that the MAP binds to the membrane or associates with a membrane-bound protein: since microtubules in an array are at most 20 nm from the membrane, steric hindrance – the MAP bumping into the membrane in some orientations – would suffice to constrain the angles of nucleated microtubules. In any case, whatever the exact details, the branching mechanism is clearly of the “anchoring” type, in the dichotomy of Sec. 1.4.

3.4 Microtubule screw-ratchet mechanism

Now I turn to collisions. It is well known that filaments that are polymerizing in a non-equilibrium fashion can exert forces on (say) a perpendicular wall via the “Brownian ratchet” mechanism [28]. Repeatedly, the wall thermally fluctuates away from the tip, this sterically allows another monomer to be added, which like a strut prevents the wall from returning to its original position. Similar Brownian notions were used to estimate the probability for one growing microtubule to cross over or under another one [76]. These estimates did not take into account the closeness of the membrane.

In fact, the microtubule adds tubulin units in a left-handed spiral fashion. Therefore, by a brownian ratchet mechanism, it will exert forces much like a left-handed screw being screwed into a solid. If it approaches another mt from the right, that screw path first encounters the blocking mt as the screw is turning downwards, and hence tends to lift the incoming mt upwards – towards the membrane, where it tends to get sterically blocked and

start depolymerizing. On the other hand, if the new mt comes in from the left, the screw path of polymerization will push it downwards where there is more room, and the crossover probability should be larger. Evidently, in the dichotomy of Sec. 1.4, this collision mechanism is of the “screw” type.

The microtubules spiral counter-clockwise (looking in the direction of growth), so it is the microtubules incident from the *left* that tend to get pushed downwards and cross over successfully. It follows that this mechanism predicts a sign of the precession $\omega < 0$, i.e. clockwise. In the experiment, 2/3 of the 15 cells shown in Fig. 1 of Ref. [73] showed a clockwise tendency, but that imbalance is not statistically significant, and was not commented by the authors.

3.4.1 Estimate of transverse ratchet force

I will make a quantitative estimate whether the ratchet force is strong enough to displace a microtubule far enough so as to cross over another one. It is estimated that, for physiological concentrations of tubulin, the available Brownian ratchet force is $\sim 30\text{pN}$; however, a lower limit is implied by buckling. The separation ℓ between points where the mt is anchored to the membrane is $\ell \sim 3\mu\text{m}$ [76]. Assuming a typical bending modulus $B \approx 20\text{ pN } \mu\text{m}^2$ for the microtubule, the buckling force is $B/D^2 \sim 2pN$. The unit added to a protofilament in each step is 8 nm long, the mt diameter is $2R = 35\text{ nm}$, and there are 13 protofilaments. Also, each turn around adds 1.5 units in length. From this it can be figured out that the tangent vector along the helix of successive addition points has longitudinal component $\sim 1.5(8\text{nm})/(2\pi R) \approx 0.12$. It follows that the transverse component of the available ratchet force is $(0.12)(2\text{pN}) \sim 0.2\text{pN}$.

What are we asking this force to do? In the time that the growing microtubule would grow the radius of the barrier microtubule, it has to be displaced sideways by its own radius so as to cross over. A typical growth speed is $v_g \approx 3.5\mu\text{m}/\text{min}$, so this time is $t \approx (R/v_g) \approx 0.3\text{s}$, and the displacement needed is $\Delta z \approx R$.

The response of the microtubule is determined by a combination of viscous drag and the microtubule bending modulus: a transverse force F_{tip} applied on the tip as a sudden step causes an initial displacement at the tip which spreads backwards. The drag on a rod of length L moving at velocity v in a fluid of viscosity η , analogous to Stokes’s formula for a sphere, is given by $F_{\text{drag}}/L = \zeta_{\perp}$ where

$$\zeta_{\perp} \equiv \frac{4\pi\eta}{-0.9 + \ln(L/R)}. \quad (6)$$

Taking $L \rightarrow \ell$ and assuming $\eta = 10^{-2}\text{Pa s}$ (ten times the viscosity of water), we get $\lambda \approx 0.06\text{pNs}/\mu\text{m}^2$. A proper treatment gives a differential equation for the displacement $z(x, t)$ along the microtubule:

$$\frac{\partial z(x, t)}{\partial t} = -\frac{B}{\zeta_{\perp}} \frac{\partial^4 z(x, t)}{\partial x^4}, \quad (7)$$

as is discussed in Ref. [77]. For our purposes, however, dimensional analysis will suffice. We expect the tip displacement to grow with time t as

$$\Delta z(t) \sim F_{\text{tip}} \left(\frac{t^3}{B\lambda^3} \right)^{1/4}. \quad (8)$$

Setting $\Delta z = R = 17.5\text{nm}$ and $t = 0.3\text{s}$ as argued above, we finally get $F_{\text{tip}} = 0.01\text{pN}$ as the minimum force needed, modulo the unknown coefficient of order unity in (8). This is just $1/20$ of the estimated transverse ratchet force, suggesting that force is strong enough to induce a significant bias in the crossover probability, depending which side the growing tube advances from. Specifically, as noted in Section 3.3.1, since the barrier microtubule is separated from the membrane, by $< 20\text{ nm} < 2R$, the crossover chance should be seriously reduced for a displacement in this direction.

3.5 Kinked-attachment mechanism

As already mentioned in Sec. 3.2 the greatest unsettled question about the plant microtubule array, from a physicist's perspective, is how does it (tend to) align almost transverse to the cell's long axis, but slightly helical? Sec. 3.2 suggested mechanisms whereby this depended on the orientational ordering of the microtubule array. Here I want to explore the alternative possibility that the orientation bias depends on *local* properties of the membrane, specifically its curvature.

3.5.1 Molecular level argument

Consider the chiral properties of gram-negative bacteria like E. Coli: they are believed to be determined by an actin homologue called MreB, which tends to wind around the cell membrane in a spiral, and seems to template the bacterial cell wall, made of peptidoglycans, somewhat as a plant cell's microtubules template its cellulose cell wall. But the MreB consists of a single bundle, not an array, so its orientation cannot be imputed to a collective effect. The membrane-binding type mechanism I suggest here could apply either to MreB or to plant microtubules.

The filament's persistence length exceeds the cell diameter; to make it wrap around the cell [see Fig. 5(a)], bending forces must be exerted on it by (I suggest) the same molecules that bind the filament. Thus we get binding points with a typical spacing ℓ (modifiable under the cell's control), with a *kink* at each binding point and straight segments in between them. We can characterize the spatial relation of the filament to the binding protein by two angles (β, α) for the incoming line, and (β', α') for the outgoing line [see Fig. 5(b,c)], where β or β' is the angle to the membrane plane, and α or α' is the direction within the membrane plane. If the binding points are equally spaced then $\beta = \beta'$ is constrained by the cell being a cylinder; for simplicity we assume $\beta = \beta'$ (and small) henceforth. A nonzero β corresponds

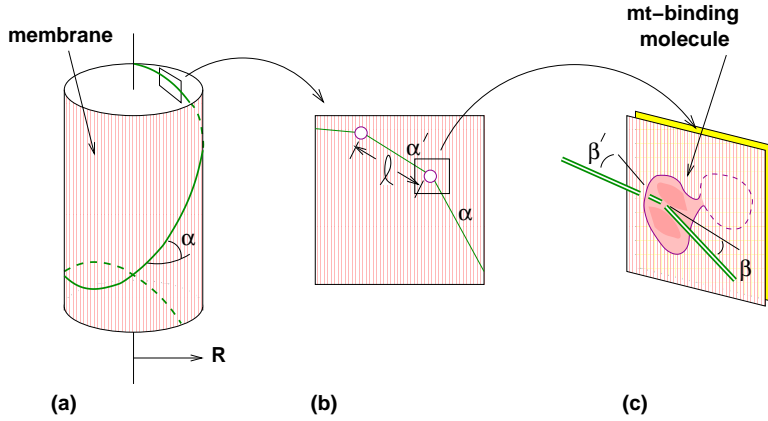


Fig. 5 Kinked-attachment mechanism for chirality of a single filament, e.g. a microtubule, (a) a cylindrical cell with the filament (heavy line) wrapped around it in a helix parametrized by a pitch angle α ; (b) zoom to a portion of the membrane: the path actually consists of straight segments between membrane-bound molecules (circles) that clasp the filament, separated by a typical spacing ℓ ; the incoming angle α need not match the outgoing angle α' (defined with respect to the filament's polarization) (c) on the molecular scale, the filament is clasped in a membrane-bound molecule, such that the filament is also bent in the direction normal to the membrane; here β and β' are the incoming and outgoing angle between filament and membrane.

to filament curvature $2\beta/\ell$, which in turn is $2\cos^2\alpha/R$, where R is the cell's radius. Thus

$$\beta(\alpha) = \frac{\ell \cos^2 \alpha}{2R}. \quad (9)$$

A certain set of angles $\{\alpha, \beta, \alpha', \beta'\}$ minimizes the binding molecule's (free) energy; any deviation from these angles has an elastic cost U which is quadratic in deviations. Locally the physics is symmetric around the membrane normal direction, so the in-layer angles enter only through the difference $\Delta\alpha \equiv \alpha' - \alpha$, but there is no reason to expect symmetry around $\Delta\alpha = 0$. Thus the form is

$$U = \frac{1}{2}K_{11}(\Delta\alpha)^2 + K_{12}\Delta\alpha(\beta - \beta_0) + \frac{1}{2}K_{22}(\beta - \beta_1)^2. \quad (10)$$

Say we are given the incoming angle α [which by (9) constrains β]: the optimum value of $\Delta\alpha$, corresponding to mechanical equilibrium, is $\Delta\alpha = -(K_{12}/K_{11})(\beta - \beta_0)$. Rewriting in differential form and substituting from (9), the end result is

$$\frac{d\alpha}{ds} = -\frac{K_{12}}{K_{11}} \frac{\ell}{4R} (\cos 2\alpha - \cos 2\alpha_0), \quad (11)$$

where α_0 is defined by $\beta(\alpha_0) \equiv \beta_0$. Eq. (11) is the desired formula for expressing the selection of a helix with a particular angle α_0 . The basic idea is that, due to the generic cross term in Eq. (10), the sense of the filament's in-plane bending is controlled by whether its out-of-plane curvature is greater or less than a threshold; that out-of-plane curvature in turn is controlled by

the pitch angle α . As a result, a filament at angle α_0 turns neither to the right nor to the left. Filaments at other angles bend within the plane of the membrane, until they are at angle α_0 . All this depends on having $K_{12} > 0$ in (10); the other sign implies a positive feedback on $\alpha - \alpha_0$, in which case the favored angle would be either 0° or 90° .

4 Brain handedness, chiral crawling and actin pitch-change

Up to now, all our examples of chirality in animals were in the context of development. I now turn to some less-developed or recent emerging stories that involve cell growth and/or motility and/or adhesion.

Perhaps the most studied asymmetry is that of the human brain, and perhaps the mechanism of its implementation is the least understood. Nerve cells migrate far in the developing brain. After stopping they extend long “neurites” (meaning axons or dendrites) which will form synapses to interconnect with other nerve cells. This growth is not so different from locomotion: either phenomenon involves chemotaxis and cytoskeletal elements pushing out the membrane.

A difficulty is that, if brain symmetry is broken at a late stage when the tissue is three-dimensional, what specifies locally the directions “ \hat{x} ” and “ \hat{z} ” which enter into a right-hand rule? In most of the other examples of L/R phenomena surveyed in this paper, the cells form a two dimensional layer, with the upper and lower sides inequivalent, so that we get one axis for free. Is it possible that brain asymmetry instead arises as a very early mechanism while the embryo is roughly two dimensional? Could this be related to the L/R mechanism which Levin [78] claims exists in vertebrates as an alternative to the cilia-driven flow?

4.1 Chirality in nerve cell growth

One possible microscopic basis for brain handedness is the noticeably chiral growth of the neurites. Originally this was observed as a tendency of neurites grown on a flat substrate to curve rightwards with a radius of curvature ~ 1 mm [80,81] or much less [82,83]. Recently, in a three-dimensional gel, it was shown the neurite tip’s motion could be idealized as a right-handed helix of radius $\sim 2\mu\text{m}$ and pitch $\sim 20\mu\text{m}$ [81]. This was shown to depend on the processive form of Myosin V, which steps in a spiraling fashion [45].

All in all, this top-level story seems very reminiscent of plant roots, (see Section 3.1, below). The turning on a flat substrate being analogous to plant roots that do the same, or that exhibit root skewing (see Section 3.1); the chemotaxis of the neurite toward its target is analogous to the gravitropism (downward bias) of the plant roots. Further understanding would benefit from mechanical studies of the neurite elasticity and forces exerted during growth, perhaps presenting artificial mechanical barriers as the three-dimensional root experiments of Ref. [54] or the microfabricated channels in the cell swarming experiments (Sec. 4.3, and 5.1, below).

Detailed studies of axon growth over time showed that the tip behaves reminiscent of the famous chemotaxis of the bacterium *E. Coli*. It follows a fixed bearing, modulo inherent angular fluctuations, for a long time; then with, a time constant ~ 4 hours, it executes a turn to a new bearing – which is chirally biased to be $\sim 30^\circ$ to the left of the old one (Ref. [84], figures 4C, 5B, and 6B).

In the case of *E. Coli*, the turn is executed by tumbling, so one wonders if the neurite’s turn might be analogously accompanied by some sharp looping twist, which could be revealed experimentally by detailed microscopy at the points of turning. Whereas *E. Coli* tumbles many times so as to randomize its new direction, the speculated looping of the neurite would have to be less than a full turn so as to keep its correlation with the preceding direction. As in all the other examples, since an up/down asymmetry is a prerequisite to distinguishing left and right within the planem, an experimental suggestion is to vary that asymmetry, perhaps by growing neurites confined on both sides. A related question is to compare conditions leading to different macroscopic radius of curvature: is this simply a change in the frequency of reorientation events, or a change in the degree of bias in each event?

On the molecular level, the next experimental step would be to address the necessity of microtubules, actin, and myosin for the bias in the turning. It would also be of interest to survey mutations known to affect brain laterality, identify any that relate to cytoskeletal genes, and then see whether the chirality of neurite growth is disrupted in the mutants.

4.2 Actin pitch-change mechanism

One way to generate torsion from actin filaments is to take advantage of the inherent elasticity of a chiral filament, which by symmetry should include a bilinear cross-coupling between the longitudinal strain and the torsion. That term has been measured in DNA [86,87]. but not yet, it seems, in actin (where it may be less important: see [88], footnote 3).

Consider a polymerizing pseudopod, made of an actin network that pushes the cell membrane as it polymerizes. Presumably, each new actin filament is under a small tension or compression. But as the actin network exerts a forwards force on the membrane, it must develop internal longitudinal stresses, which due to the cross-coupling induce a torque of the same sense in each filament. Since these filaments are cross-linked they cannot unwind freely, and the network has a macroscopic torsion. Inside an approximately planar cell crawling on a surface, this would tend to twist the pseudopod out of that plane. Granting that the “upper” (free) and “lower” (surface-bound) sides of the cell are inequivalent, the twist converts this to a left-right inequivalence. If the actin network experiences a different chemical environment as it matures, so as to change the preferred pitch, we get the same outcome. One would thus predict that eukaryotic cells, in chemotaxis, would walk systematically offset from the gradient direction of the attractant chemical.

No significant offset in the angle of chemotaxis has never been reported [89]. Recently, however, a chiral offset was found in animal cells when a spatially *uniform* concentration of attractant is increased. Such a step in

time is known to induce a spontaneous polarity, as defined by the nucleus-centrosome axis, and it turns out that the new axis is mainly $\sim 90^\circ$ to the left of the old one [79]. However, this behavior was shown to depend on *microtubules*, which was not found to date in any of the other animal-cell stories. It would obviously make sense to check experimentally for the involvement of myosin and/or of actin polymerization. Since different cell types display opposite handedness in channels (Sec. 4.3.2, below), one would also be curious whether they also display opposite rotations of the polarization axis.

4.3 Collective chiral crawling

Very recently, massive chirality was found in mature, motile mammalian cells. Cells were packed into micropatterned planar channels, and the layers near the walls were found to move with opposite senses on either side, like automobile traffic on a road; whether the cells “drive” on the right or the left depends on the cell type, and even on whether they are cancerous [90]. This only occurs at high packing densities of the cells, so it must be a collective effect of their interactions, presumably related to cell-cell adhesion.

4.3.1 Collective level: chiral medium?

Strikingly, the cells showed a biased motion in annuli as well as in straight channels, but not in a space shaped like an open disk. If the bias were attributed to a direct interaction of cells sensing the wall [90], flow along the edge would be seen even in the dilute limit of random-walking single cells, and it would not depend on the opposite boundary; that is what swarming bacteria do (Sec. 5.1. Instead, I conjecture that the mammalian cells are actually reacting to each other, developing a chiral stress. In the middle of the swarm, this stress is uniform so its effects cancel and nothing is seen; but adjacent to walls, it is unbalanced and drives the flow.

Thus the collective story seems fully analogous to that of the actomyosin layer in Sec. 2.4. In place of filaments, the active units here are cells, but the essential fact is the same: nearby units have an interaction which tends to orbit them in a particular sense. I would speculate that the coarse-grained flow of a cell population is described by the same continuum theory presented in Sec. 2.3.

One likely experimental test of this, as in Sec. 2.3, would be to analyze video images by cross-correlating the density fluctuation gradients with velocity fluctuations. The images show several “convection rolls” spaced around the annulus, so the first check would be to see if the cores of these rolls have a different cell density. This system offers additional opportunities to control density gradients, in the form of the wall constraints imposed by the fabricated channel geometry. If the continuum theory correctly predicts the absence of rotation in an open disk, it should also predict the differences between a variety of other shapes of the accessible region.

As noted above, I am suggesting that the cells are *not* recognizing the walls, but only each other; the walls act as purely mechanical boundary conditions. That could be tested experimentally by modifying the wall surfaces:

the prediction is that treating them with signals would have less effect than changing their coefficient of friction.

4.3.2 Cell level story: inter-cellular forces and actin polymerization?

What future experiments might uncover the rules governing the motions of individual cells and interacting pairs? One obvious fact, following the dictum in Sec. 1.3.1, is that the cells must know the difference between up and down in order to tell the difference between left and right. Presumably gravity is a minor effect, so if the cells were equally in contact with the “floor” and “ceiling” of their channels, there should be no right/left bias. Actually, a cancellation in that case follows from basic symmetry so it is predicted for any mechanism; but manipulations of the up/down differences could reveal which kind of difference is salient for the chiral flow, which would in turn be a clue for the mechanism at the next lower level.

The nicest way to unravel the cell interactions would be to use a mixture of two cell types.² One would independently vary (i) how they recognize each other (ii) whether they are right or left biased cell types. By examining the dynamics of individually imaged cells, one can distinguish between various candidate interactions which would all give the same collective behavior in a uniform system.

At the molecular level, experiment already showed that the mechanism does not require microtubules, but does depend on actin polymerization, as it is suppressed by the polymerization inhibitors latrunculin and cytochalasin [90]. Furthermore it is found *not* to depend on myosin (Ref. [90], Fig. S5). Hence the mechanism must be different from the actomyosin story of Sec. 2; instead, it presumably involves the basic cell motility, which certainly depends on actin polymerization. Thus, one possibility is to impute the mechanism to something like the actin pitch-change mechanism of Sec. 4.2.

Since I argued the handedness in this system lies in cell-cell interactions, that might suggest testing for the involvement of cadherins, involved with cell-cell adhesions. Cadherins were actually implicated in a mechanism for *Drosophila* (but with immotile cells in that case: see Sec. 4.4).

4.4 Chirality in flies

In the highly studied development of the fruit fly *Drosophila*, a small (non-functional?) chirality is manifested as looping of their guts and genitals [91, 92, 93]. This appeared at a late, many-cell stage and was shown to depend on the motor protein “unconventional” myosin type I D, as well as myosin I C; Mutants in which either I D is nonfunctional, or else I C is overexpressed, show a reversed handedness; thus it appears the respective myosins are antagonists. I include this topic because a new experiment [94] found clues which may be sufficient information for us to start (speculatively) modeling that system.

² I am grateful to Victor Luria for this suggestion.

4.4.1 Top level story: tissue shear

Namely, it found that the epithelial (tissue layer) cells lining the gut exhibit a form of chirality that I have not mentioned up to now. The packing of the cells has a preferred axis (anterior to posterior) and then this tissue gets sheared, such that cell walls transverse to that axis are biased to tilt at a nonzero angle, as idealized in figure 6. This macroscopic shear breaks right-left and up-down mirror symmetries, but does not in itself break inversion symmetry, and thus does not distinguish left and right directions. If, though, there were a preexisting anterior (head-wards) polarization, such a shear would generate a rightwards polarization.

Ref. [94] also found that cadherins – membrane proteins that mediate cell-cell adhesion and modify the stress tensor – preferentially localize on cell boundaries with (two-dimensional) normal vectors oriented in the first and third quadrants, roughly the (1,1) vector in the plane, as represented in Fig. 6(a). In the inversion mutant this preference is reversed; in a mosaic tissue where both types of cells are mixed randomly, each category of cell boundary has a cadherin preference which is the mean of that for the cell types on either side. As recognized in Ref. [94], the extra cadherins on boundaries normal to the (1,1) direction drive a cortical tension and contraction normal to (1,1), as shown in Fig. 6(b). When – as in the hindgut – the tissue is rolled into a tube, this shear drives a spiral twist of the tube, as verified in Ref. [94] by a toy simulation. Thus, the top level of the L/R mechanism – represented by continuum elasticity – is qualitatively understood.

Furthermore, when the investigators engineered a mixture of the wild-type (+) and the reversal mutant (–) cells, they showed that cadherin was distributed on the (++) type walls with the same bias as in wild type, but the (--) walls were biased the opposite way, and the (+-) walls were not significantly biased, as shown in Fig. 6(c).

4.4.2 Cell-level mechanism: biased transport

At the molecular level, myosins I C and I D are known to transport vesicles (small membrane bags) containing proteins – perhaps the cadherins – along actin fibers. Thus we need a mechanism for biased transport. A possibly useful fact is that the mutants with inverted handedness do *not* have a reversal in the physical bias of the transport, but rather in the sign of the signal which gets transported [94]. Ref. [92] already recognized that either the actin filaments are aligned exactly along the anterior/posterior axis but the myosin transport is biased, or else the fibers themselves are turned. I will describe slightly more explicit candidate mechanisms corresponding to each of these possibilities.

The first candidate mechanism is “asymmetric transport” which I worked out in Sec. 3 of Ref. [6] for purely pedagogical purposes, whereby a filament array oriented bidirectionally along the A/P axis *without* L/R bias, does transport vesicles with a diagonal bias. The first condition for this is easy enough: a helical bias in the myosin I D step, similar to the myosin II that is better known and discussed in Sec. 2.4, above. The second condition is

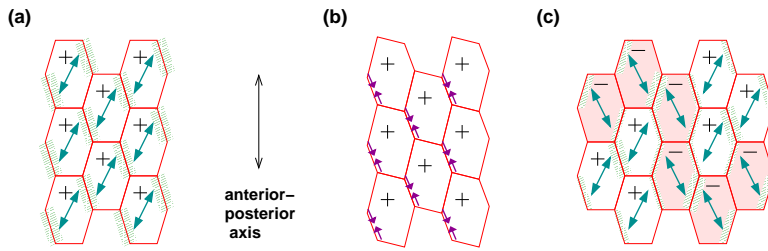


Fig. 6 Left-right asymmetry in hindgut epithelial tissue of *Drosophila*. (inspired by Ref. [94]). In this cartoon, emphasizing the asymmetries, cells are represented as elongated hexagons, omitting the irregularities of the actual tissue (shown in Ref. [94], Figures 2 and 3). (a) In the wild-type (cells with +) cadherin (DE-Cad, shown by hatching) is observed to be localized on the walls tilted leftwards from the anterior-posterior (AP) axis; this is attributed to a hypothetical myosin-based transport of vesicles along the arrowed directions. (b) In the final tissue, the orientation of walls has a systematic bias (i.e. the tissue is sheared); this is attributed to contraction caused by the cadherin (opposing arrows). (c) In a tissue mixing wild-type (+) cells with mutant (-, shaded) cells, the cadherin density along each cell wall is the sum of the densities attributable to the respective adjoining cells.

that the fibers are flush against a membrane which sterically constrains the tendency of the vesicles to spiral around the actin as they are pulled by myosin I D. For this mechanism to give a non-cancelling result, the A/P polarized array of actin filaments must sit on one large surface of the cell (say the upper one) but not the other.

As an alternative candidate mechanism, one could posit a large scale flow of a cortical actomyosin layer as in Sec. 2, which will tend to run counter-clockwise next to the cell boundaries, as we look down on the upper cell faces. If the transporting actin array has its endpoints embedded in that cortical layer, the array's orientation tends to precess with that layer, just as I posited the microtubule array does in plant cells (Sec. 3.2). Just as in that story, if this precession is combined with a competing pull towards a particular axis (here the A/P axis), the result will be a static orientation with a mean tilt. But as with the asymmetric-transport mechanism, the key question is: why either the top or the bottom face of the cell dominates over the other one? I would suggest that further experiments focus on the up/down difference.

Based on the above speculations, it seems fairly plausible that the mechanism in *Drosophila* – whatever it is – belongs to the “linear response” category of Sec. 1.5, and not to the more common “symmetry breaking” category.

5 Bacteria

Bacteria exhibit a number of handed phenomena that are naturally handled under the same framework as multicellular organisms. Of course, there is not (necessarily) an inter-cellular level here, but even in single cells one needs the same multiple levels of description (see below). An important motivation for me to include this (very incomplete) sketch about bacteria is that they are the subject of the best-developed existing theory that applies to left/right

phenomena the sort of multiscale approach that I am espousing in this paper. Such treatments are usually set up at the level of mechanics or fluid dynamics.

5.1 Flagellated bacteria

It is already well-known that in flagellated bacteria, such as *E. Coli*, there is a hydrodynamic interaction of the flagella with nearby walls that drives a biased turning of the bacterium's path around the axis of the wall normal [95]. It was found that *E. Coli* in microchannels swim on the right as *isolated* cells, [96] thus indicating a relatively trivial non-cooperative reason for the observed chiral swarming motions [97], as opposed to the collective origin I conjectured for the chiral swarming of mammalian cells (Sec. 4.3).

Flagellated bacteria are also long known to form chiral colony patterns on agar gels [98] and this has been understood theoretically in terms of their single-cell dynamics on a surface [99].

Later, a continuum theory [100] was written down aiming to model this growth, using a precessing orientation field similar in meaning to my $\theta(\mathbf{r})$ from the plant microtubule arrays (Sec. 3). Simulations of these equations produce feather-like chiral patterns similar to the bacterial colonies; tip-splitting instabilities are central to this pattern formation.

5.2 Non-flagellated bacteria and their cytoskeleton

I now turn to bacilli (rod shaped bacteria) without heavy cell walls such as *B. subtilis* or *Caulobacter*. Independent of whether they have flagella, many species adopt naturally handed spiral shapes; mutants do in the cases of *B. Subtilis* [101] or *E. Coli* [102]. The external shape presumably depends on the organization of the layer of peptidoglycans that form a cell wall outside the membrane. It is believed that the actin homolog MreB, which forms a single helical bundle just inside the membrane, right-handed in *B. subtilis* [103] or left-handed in *E. Coli* [104], directs the wall synthesis [104,105]. Thus the story is reminiscent of plant cells, in which the cellulose synthesis (forming the cell wall) is directed by the microtubules, which organize helically inside the membrane, as I discussed at length in Sec. 3.

One reason to bring up this system is that it demonstrates that it not necessary to form a collective state in order to bias the sense of the helix, which suggested to me the likelihood of something like the "kinked-attachment" mechanism of Sec. 3.5.1. Also, we see it is not essential to have inter-cellular interactions in order to encounter multiple levels of description: filament polymerization dynamics at the bottom, perhaps a statistical description of the cell wall and its continuum theory as an intermediate level, and mechanics determining external shape at the top level.

Existing theory is often based on the notion of twist-to-writhe conversion: if you twist a rod, differential geometry shows the strain is partially reduced when the centerline becomes helical, and this may be the mechanically stable state. Ref. [106] addresses how an existing spiral in the cylindrical cell can, by elongating and pressing against the end caps, drive the external shape to

a spiral. Ref. [104] contains a different theory based, more plausibly, on the helical correlations built into the peptidoglycan wall, because its new strands are nucleated from the MreB filament.

Another macroscopic – or intercellular – level handedness is the long-known supercoiling of the strands of cells formed when mutant *B. Subtilis* cells divide without separating [107]. This hints at a more microscopic origin similar to the division-twist posited in snail embryose (Sec. 2.2). There is an analogy to the micro level in which each linked cell in a strand corresponds to a monomer in a cytoskeletal filament.

Turning to the molecular level, but still in the spirit of the twist-to-writhe conversion, Ref. [108] has explained why the MreB filament forms a helix within the cell. They treat the MreB as a ribbon that, like DNA, has an inherent twist, and that attaches to the membrane with its flat side parallel. Notice that – unlike most other mechanisms mentioned at this level – this is a pure mechanical equilibrium theory of passive elements, that does not depend on polymerization or any other driven behavior. It has been shown that MreB forms a two-strand helix – so it really is a ribbon – furthermore MreB binds directly to the membrane without need for a linker [109] Hence, for the case of MreB Ref. [108] appear to have the correct molecular picture as opposed to the “kinked-attachment” one in Sec. 3.5.

6 Discussion and conclusions

In this speculative review, I have asserted it is helpful to approach left/right asymmetries in disparate biological systems in parallel, with a common framework, rather than in a compartmentalized fashion. To illustrate this, I discussed, or at least mentioned, the following examples:

- node cilia in vertebrates (Sec. 1.1.1);
- actomyosin, in snail embryos and also in *C. elegans* (Sec. 2)
- the microtubule layer in plant cells (Sec. 3);
- neurites, perhaps ultimately the human brain (Sec. 4.1);
- collective swarming by motile mammalian cells (Sec. 4.3)
- chirality of cell packing in *drosophila* (Sec. 4.4).
- bacteria with the actin homolog MreB (Sec. 5);

(Sec. 3.1 also very briefly mentioned the spiral growth of the fungus *Phycomyces*; this would be very attractive to develop as another example.)

I have talked about general principles, and presented several examples, of how chiral information gets from the molecular scale to the macro scale, so that (almost) all individuals break left/right symmetry in the same ways. Each story naturally unfolds on multiple length scales: there is always an intracellular story and an organism level story, and sometimes more than two levels. So far, all the mechanisms imagined, and all those observed, involve the cytoskeleton (microtubules or actin filaments) at the molecular level.

Just how can the molecular chirality affect larger scale dynamics? In Sec. 1.4, I identified two general ways. The first is a “screw” mechanism, meaning motion *along* a long helical fiber gets converted into rotation *around*

the fiber, due e.g. to a motor's walking, the collisions of a helically polymerizing microtubule, or to the fiber's twist/extension cross-coupling. (This feels attractive to physicists since it uses the translational invariance of the long fiber and its inherent chirality.)

The second mechanism is the “membrane-anchoring” mechanism: some membrane-bound molecule also specifically binds the fibers in a particular orientation. (This scenario will feel more familiar to biologists.) The membrane-anchoring mechanism furnishes a hint for genetic or protein-expression studies as to the existence, or the importance, of such a protein.

@1 Symmetry principles (Sec. 1.3) called for, in any L/R mechanism and at any level, not only a chiral element but also two axes. But in the majority of examples given above, where we have a glimmer of understanding, we find a screw mechanism giving rise to a it only produced a handed rotating tendency in the dynamics of this array: a “relative” chirality, in the categories of Sec. 1.4: This was the case for the shearing actomyosin layer, (Sec. 2.3), or the orientationally precessing microtubule arrays. (Sec. 3.2). In these cases, the conjectured cell-level mechanism is easier to implement since it requires only *one* pre-existing axis – the membrane normal or cell layer normal, depending on what level we are at. To produce a macroscopic handedness, this rotating dynamics must occur in the context of some larger-scale nonuniformity – the furrow between dividing animal cells, or the curvature directions and end caps of a plant cell –

It is also striking that the top level story usually involves mechanics. This may be ascribed to how L/R asymmetry is represented: we ultimately need “positional information”, meaning each cell has access to a signal which tells which side of the L/R line it is on, but the lower level mechanisms typically produce local *polarization* of the cells. Mechanics is a convenient way to convert that to a macroscopic distortion, an operation which is a bit like inverting the derivative in calculus (as I commented in Sec. 1.3.3 of Ref. [6]). The other way to convert orientational information to positional information is by using polarized, driven transport to build up a gradient of some signal. The only instances of that are transport by the surrounding fluid, at the top level of the nodal-flow story of vertebrates (Sec. 1.1.1) or in the likely vesicle transport, in the cell-level story of flies (Sec. 4.4.2).

I have given, where I could, a few experimental productions, or I pointed out experiments which would clarify a mechanism. The recurring theme in these suggestions, in all the different examples, correlates with the above observation that chirality develops in layers. Thus, we need experiments to unravel what aspect of the up/down asymmetry of such layers controls the left/right asymmetry within them: any such discoveries will be clues for the left/right mechanism.

It is left for future research to turn all these ideas into quantitative estimates, a necessary condition before any physics may be considered as completed.

Acknowledgments I thank S. Grill, T. Hashimoto, F. Jülicher, M. Levin, V. Luria, N. Sanjana, S. Seung, E. D. Siggia, G. O. Wasteneys, N. Wingreen, R. Chachra, and J. X. Shen, for discussions and communications (and the

last two for collaborations). This work was supported by the U.S. Dept. of Energy, grant DE-FG-ER45405.

References

1. N. A. Brown and L. Wolpert, *Development* 109, 1-9 (1990), "The development of handedness in left/right asymmetry".
2. W. B. Wood, *Annu. Rev. Cell. Dev. Biol.* 13, 53-82 (1997), "Left-right asymmetry in animal development."
3. M. Levin, *Mech. Dev.* 122, 3-25 (2005) "Left-right asymmetry in embryonic development: a comprehensive review".
4. W. B. Wood, *PLoS Biology* 3, e292 (2005), "The left-right polarity puzzle: determining embryonic handedness."
5. A. R. Palmer, *Science* 306, 828-833 (Oct. 2004). "Symmetry breaking and the evolution of development."
6. C. L. Henley, pp. 54-61 in *Advances in Theoretical Physics*, ed. V. Lebedev and M. Feigel'man, AIP Conf. Proc. No 1134 (Melville, NY, 2009). (Proc. Landau 100 Memorial Conf., Chernogolovka, June 2008). "Possible mechanisms for initiating macroscopic left-right asymmetry in developing organisms".
7. F. C. Frank, *Biochim. Biophys. Acta* 11, 459-464 (1953), "On spontaneous asymmetric synthesis."
8. V. A. Avertisov, V. I. Goldanskii, and V. A. Kuz'min. *Physics Today*, July 1991, pp 33-41, "Handedness, origin of life, and evolution".
9. J. Cooke, *Biol. Rev.* 79, 377-407 (2004), "Developmental mechanism and evolutionary origin of vertebrate left/right asymmetries"
10. N. Hirokawa, Y. Tanaka, Y. Okada, and S. Takeda *Cell* 125, 33-45 (Apr 7, 2006). "Nodal Flow and the Generation of Left-Right Asymmetry."
11. C. McManus, *Right hand, left hand: the origins of asymmetry in brains, bodies, atoms, and cultures* (Harvard Univ. Press, Cambridge MA, 2002), and references therein.
12. S. Nonaka, Y. Tanaka, Y. Okada, S. Takeda, A. Harada, Y. Kanai, M. Kido, and N. Hirokawa, "Randomization of leftright asymmetry due to loss of nodal cilia generating leftward flow of extraembryonic fluid in mice lacking KIF3B motor protein", *Cell* 95, 829837 (1998).
13. J.H.E. Cartwright, O. Piro, and I. Tuval, *PNAS* 101, 7234-7239 (2004), "Fluid-dynamical basis of the embryonic development of left-right asymmetry in vertebrates".
14. H. Hamada, C. Meno, D. Watanabe and Y. Saijoh, *Nature Reviews Genetics* 3, 103-113 (2002), "Establishment of vertebrate left-right asymmetry".
15. S. Nonaka, H. Shiratori Y. Saijoh, and H. Hamada, *Nature* 418, 96-99 (2002), "Determination of left-right patterning of the mouse embryo by artificial nodal flow."
16. M. Levin, *Crit. Rev. Oral Biol. Med.* 15, 197-206 (2004), "The embryonic origins of left-right asymmetry."
17. D. S. Adams, K. R. Robinson, T. Fukumoto, S. Yuan, R. C. Albertson, P. Yelick, L. Kuo, M. McSweeney, and M. Levin, *Development* 133, 1657-1671 (2006). "Early, H⁺-V-ATPase-dependent proton flux is necessary for consistent left-right patterning of non-mammalian vertebrates"
18. S. Aw, D. S. Adams, D. Qiu, and M. Levin, *Mech. Devel.* 125, 353-372 (2008), "H,K-ATPase protein localization and Kir4.1 function reveal concordance of three axes during early determination of left-right asymmetry."
19. W. B. Wood, *Nature* 349, 536-8 (1991). "Evidence of handedness in *C. Elegans* embryos for early cell interactions determining cell fates."
20. R. J. Poole and O. Hobert, *Current Biology* 16, 2279-2292 (2006), "Early embryonic patterning of neuronal left/right asymmetry in *C. elegans*."
21. T. Sun and C. A. Walsh, *Nature Revs. Neuroscience* 7, 655 (2006), "Molecular approaches to brain asymmetry and handedness."

-
22. Y. B. Malashichev and R. J. Wassersug, *Bioessays* 26, 512-22 (2004), "Left and right in the amphibian world: which way to develop and where to turn?"
 23. Ye. B. Malashichev and A. W. Deckel, ed., *Behavioral and morphological asymmetries in vertebrates* (Landes Bioscience, Georgetown TX, 2006).
 24. M. E. Halpern, J. O. Liang, and J. T. Gamse, *Trends Neurosci.* 26, 308-313 (2003), "Leaning to the left: laterality in the zebrafish forebrain."
 25. R. Kawamura, A. Kakugo, K. Shikinaka, Y. Osada, and J. P. Gong, "Ring-shaped assembly of microtubules shows preferential counterclockwise motion", *Biomacromolecules* 9, 2277 (2008).
 26. G. M. Grason and R. F. Bruinsma, *Phys. Rev. Lett.* 99, 098101 (2007) [4 pages], "Chirality and Equilibrium Biopolymer Bundles".
 27. T. Okumura, H. Utsuno, J. Kuroda, E. Gittenberger, T. Asami, and K. Matsuno, *Developmental Dynamics* 237, 3497-3515 (2008), "The development and evolution of left-right asymmetry in invertebrates: lessons from *Drosophila* and snails".
 28. C. S. Peskin, G. M. Odell, and G. F. Oster. "Cellular motions and thermal fluctuations: the Brownian ratchet." *Biophys. J.* 65:316-324 (1993).
 29. Y. Shibazaki, M. Shimizu, and R. Kuroda, *Current Biology* 14, 1462-1467 (2004), "Body handedness is directed by genetically determined cytoskeletal dynamics in the early embryo"
 30. R. Kuroda; B. Endo, M. Abe, and M. Shimizu, *Nature* 462, 790-794 (2009), "Chiral blastomere arrangement dictates zygotic left-right asymmetry pathway in snails"
 31. C. Pohl and Z. Bao, *Devel. Cell.* 19, 402-412 (2010), "Chiral forces organize left-right patterning in *C. elegans* by uncoupling midline and anteroposterior axis".
 32. M. L. Manning, R. A. Foty, M. S. Steinberg, and E.-M. Schoetz, *PNAS* 107, 12517 (2010), "Coaction of intercellular adhesion and cortical tension specifies tissue surface tension".
 33. I. Mabuchi, *J. Cell Science* 107, 1853-1862 (1994), "Cleavage furrow: timing of emergence of contractile ring filaments and establishment of the contractile ring by filament bundling in sea urchin eggs."
 34. T. Kamasaki, M. Osumo, and I. Mabuchi, *J. Cell Biol.* 178, 765-771 (2007), "Three-dimensional arrangement of F-actin in the contractile ring of fission yeast".
 35. G. Salbreux, J. Prost, and J. F. Joanny, *Phys. Rev. Lett.* 103, 058102 (2009), "Hydrodynamics of Cellular Cortical Flows and the Formation of Contractile Rings".
 36. J. A. Åström, S. von Althaus, P. B. Sunil Kumar, and Mikko Karttunen, *Soft Matter* 6,5375-5381 (2010), "Myosin motor mediated contraction is enough to produce cytokinesis in the absence of polymerisation".
 37. See movie 3 in "Asymmetric cell division and axis formation in the embryo", by Pierre Gönczy and Lesilee S. Rose, in *WormBook*, http://wormbook.org/chapters/www_asymcelldiv/asymcelldiv.html.
 38. M. V. Danilchik, E. E. Brown, and K. Riepert, *Development* 133, 4517-4526 (2006), "Intrinsic chiral properties of the *Xenopus* egg cortex: An early indicator of left-right asymmetry?"
 39. S. Fürthauer, M. Stempel, S. W. Grill, and F. Jülicher, "Generic theory of active chiral fluids", in preparation.
 40. M. Stempel, S. Fürthauer, S. W. Grill, and F. Jülicher, "Thin Films of Chiral Motors", arXiv:1112.3492.
 41. M. Mayer, M. Depken, J. Bois, F. Jülicher, and S. W. Grill, "Anisotropies in cortical tension reveal the physical basis of polarizing cortical flows" *Nature*, 467, 617-621 (2010).
 42. J. F. Beausang, H. W. Schroeder, P. C. Nelson, and Y. E. Goldman, "Twirling of Actin by Myosins II and V Observed via Polarized TIRF in a Modified Gliding Assay", *Biophys. J.* 95, 5820-5831 (2008).
 43. T. Nishizaka, T. Yagi, Y. Tanaka, and S. Ishiwata, *Nature* 361:269-271 (1993). "Right-handed rotation of an actin filament in an in vitro motile system".

44. A. Vilfan, *Biophys. J.* 97, 1130 (2009), "Twirling Motion of Actin Filaments in Gliding Assays with Nonprocessive Myosin Motors".
45. M. Y. Ali, *Nature Struc. Biol.* 9, 464 (2002), "Myosin V is a left-handed spiral motor on the right-handed actin helix".
46. N. Morone, T. Fujiwara, K. Murase, R. S. Kasai, H. Ike, S. Yuasa, J. Usukura, and A. Kusumi, "Three-dimensional reconstruction of the membrane skeleton at the plasma membrane interface by electron tomography", *J. Cell. Biol.* 174, 851-862 (2006)
47. C. R. Cowan and A. A. Hyman, "Acto-myosin reorganization and PAR polarity in *C. elegans*". *Development* 134, 1035-1043 (2007).
48. D. Vavylonis, J.-Q. Wu, S. Hao, B. O'Shaughnessy, and T. D. Pollard, *Science*, 319, 97-100 (2008), "Assembly Mechanism of the Contractile Ring for Cytokinesis by Fission Yeast"
49. F. Ziebert and I. S. Aranson, *Phys. Rev. E* 77, 011918 (2008)[5pp], "Rheological and structural properties of dilute active filament solutions".
50. Y. Nakadera, C. Sutcharit, T. Ubukata, K. Seki, H. Utsuno, S. Panha, and T. Asami, *J. Evol. Biol.* 23, 2377-2384 (2010) "Enantiomorphs differ in shape in opposite directions between populations"
51. T. Hashimoto and T. Kato, *Curr. Opinion in Plant Biol.*, 9, 5-11 (2006), "Cortical control of plant microtubules".
52. S. Thitamadee, K. Tuchiya, and T. Hashimoto, *Nature* 417, 193 (2002), "Microtubule basis for left-handed helical growth in *Arabidopsis*;"
53. T. Ishida, Y. Kaneko, M. Iwano, and T. Hashimoto, *PNAS* 104, 8544-8549 (2007), "Helical microtubule arrays in a collection of twisting tubulin mutants of *Arabidopsis thaliana*"
54. J. L. Silverberg, R. D. Noar, M. S. Packer, M. J. Harrison, C. L. Henley, I. Cohen, and S. J. Gerbode, in preparation.
55. M. V. Thompson and N. M. Holbrook, *Plant Pathology* 135, 1822-1837 (2004). "Root-gel interactions and the root waving behavior of *Arabidopsis*"
56. T. Hashimoto, personal communication.
57. M. P. Wold and R. I. Gamow, *J. Theor. Biol.* 159, 39-51 (1992), "Fiber-composite model for helical growth in the *Phycomyces* cell wall".
58. R. Dixit and R. Cyr, *Plant Cell* 16, 3274-1350 (2004), "Encounters between dynamic cortical microtubules promote ordering of the cortical array through angle-dependent modifications of microtubule behavior".
59. D. W. Ehrhardt, *Curr. Opinion Cell Biol.* 20, 107-116 (2008), "Straighten up and fly right-microtubule dynamics and organization of non-centrosomal arrays in higher plants".
60. S. L. Shaw, R. Kamyar, and D. W. Ehrhardt, *Science* 300, 1715-18 (2003), "Sustained microtubule treadmilling in *Arabidopsis* cortical arrays."
61. E. Kawamura and G. O. Wasteneys, *J. Cell. Sci.* 121, 4114 (2008) "MOR1, the *Arabidopsis* homologue of *Xenopus* MAP215, promotes rapid growth and shrinkage, and suppresses the pausing of microtubules in vivo".
62. J. Chan, A. Sambade, G. Calder, and C. Lloyd, *Plant Cell* 21, 2298-306 (2009), "*Arabidopsis* cortical microtubules are initiated along, as well as branching from, existing microtubules",
63. V. A. Baulin, C. M. Marques, and F. Thalmann, *Biophys. Chemistry* 128, 231-244 (2007), "Collision induced spatial organization of microtubules".
64. R. J. Hawkins, S. H. Tindemans, and B. M. Mulder, *Phys. Rev. E* 82, 011911 (2010), "Model for the orientational ordering of the plant microtubule cortical array".
65. S. H. Tindemans, R. J. Hawkins, and B. M. Mulder, *Phys. Rev. Lett.* 104, 058103 (2010), "Survival of the aligned: ordering of the plant cortical microtubule array".
66. J. F. Allard, G. O. Wasteneys, and E. N. Cytrynbaum, *Mol. Biol. Cell.* 21, 278-286 (2010), "Mechanisms of self-organization of cortical microtubules in plants revealed by computational simulations".
67. X-Q Shi and Y-Q Ma, *PNAS* 107, 11709-14 (2010), "Understanding phase behavior of plant cell cortex microtubule organization".

-
68. E. C. Eren, R. Dixit, and N. Gautam, *Mol. Biol. Cell.* 21, 2674-84 (2011), "A three-dimensional computer simulation model reveals the mechanisms for self-organization of plant cortical microtubules into oblique arrays".
 69. E. E. Deinum, S. H. Tindemans, and B. M. Mulder, *Phys. Biol.* 8, 056002 (2011), "Taking directions: the role of microtubule-bound nucleation in the self-organization of the plant cortical array".
 70. E. C. Eren, N. Gautam, and R. Dixit, "Computer Simulation and Mathematical Models of the Noncentrosomal Plant Cortical Microtubule Cytoskeleton", *Cytoskeleton* 69, 144154 (2012).
 71. J. X. Shen and C. L. Henley, unpublished.
 72. C. Ambrose, J. F. Allard, E. N. Cytrynbaum, and G. O. Wasteneys, *Nature Communications* 2, 430 (2011) [12 pp].
 73. J. Chan, G. Calder, S. Fox, and C. Lloyd, *Nature Cell Biol.* 9, 171 (2007), "Cortical microtubule arrays undergo rotary movements in *Arabidopsis* hypocotyl epidermal cells".
 74. G. O. Wasteneys and J. C. Ambrose, *Trends in Cell Biol.* 19, 62-71 (2009), "Spatial organization of plant cortical microtubules: close encounters of the 2D kind".
 75. R. D. Preston, *Planta* 155, 356-363 (1982), "The case for multinet growth in growing walls of plant cells".
 76. J. F. Allard, J. C. Ambrose, G. O. Wasteneys, and E. N. Cytrynbaum, *Biophys. J.* 99, 1082-90 (2010), "A mechanochemical model explains interactions between cortical microtubules in plants".
 77. C. H. Wiggins and R. E. Goldstein, *Phys. Rev. Lett.* 80, 3879 (1998), "Flexive and propulsive dynamics of elastica at low Reynolds number".
 78. M. Levin, *Birth Defects Research (C)* 78, 191-223 (2006), "Is the early left-right axis like a plant, a kidney, or a neuron? The integration of physiological signals in embryonic asymmetry".
 79. J. Xu, A. van Kaymeulen, N. M. Wakida, P. Carlton, M. W. Berns, and H. R. Bourne, "Polarity reveals intrinsic cell chirality", *PNAS* 104, 9296-9300 (2007).
 80. A. M. Heacock and B. W. Agranoff *Science* 198: 64-66. (1977) "Clockwise growth of neurites from retinal explants"
 81. A. Tamada, S. Kawase, F. Murakami, and H. Kamiguchi, *J. Cell. Biol.* 188, 429-441 (2011), "Autonomous right-screw rotation of growth cone filipodia drives neurite turning".
 82. H. F. Romijn, M. T. Mud, P. S. Wolters, and M. A. Corner, *Brain Research* 192: 575-580 (1980), "Neurite formation in dissociated cerebral cortex in vitro: evidence for clockwise outgrowth and autotopic contacts."
 83. J. Hagmann, D. Dagan, A. I. Matus, and I. B. Levitan, *J. Neurobiol.* 23:354-363 (1992), "Directional control of neurite outgrowth from cultured hippocampal neurons is modulated by the lectin concanavalin A".
 84. N. E. Sanjana, Ph. D. thesis (M. I. T., 2010) "Quantitative analysis of axon elongation: a novel application of stochastic modeling techniques to long-term, high-resolution time-lapse microscopy of cortical neurons": URL dspace.mit.edu/bitstream/handle/1721.1/58281/639302908.pdf.
 85. N. E. Sanjana and H. S. Seung, personal communication.
 86. T. Lionnet, S. Joubaud, R. Lavery, D. Bensimon, and V. Croquette, *Phys. Rev. Lett.* 96, 178102 (2006), "Wringing Out DNA".
 87. J. Gore, Z. Bryant, M. Nöllmann, M. U. Le, N. R. Cozzarelli, and C. Bustamante, *Nature* 442, 836 (2006), "DNA overwinds when stretched."
 88. R. D. Kamien, T. C. Lubensky, P. Nelson, and C. S. O'Hern, "Direct determination of DNA twist-stretch coupling", *Europhys. Lett.* 38, 237-242 (1997).
 89. C. Arriemerlou and T. Meyer. "A Local Coupling Model and Compass Parameter for Eukaryotic Chemotaxis" *Developmental Cell* 8: 215-227 (2005).
 90. L. Q. Wan, K. Ronaldson, M. Park, G. Taylor, Y. Zhang, J. M. Gimble, and G. Vunjak-Novakovic, *PNAS* 108, 12295-12300 (2011), "Micropatterned mammalian cells exhibit phenotype-specific left-right asymmetry".
 91. P. Spéder, G. Adam, and S. Noselli, *Nature* 440, 803-807 (Apr. 2006), "Type II unconventional myosin controls left-right asymmetry in *Drosophila*".

-
92. S. Hozumi, R. Maeda, K. Taniguchi, et al. *Nature* 440, 798-802 (2006), "An unconventional myosin in *Drosophila* reverses the default handedness in visceral organs".
 93. P. Spéder and S. Noselli, *Curr. Opin. Cell Biol.* 19, 82-87 (Feb. 2007), "Left-right asymmetry: class I myosins show the direction".
 94. K. Taniguchi, R. Maeda, T. Ando, T. Okumura, N. Nakazawa, R. Hatori, M. Nakamura, S. Hozumi, H. Fujiwara, and K. Matsuno, *Science* 333, 339 (2011), "Chirality in planar cell shape contributes to left-right asymmetric epithelial morphogenesis".
 95. W. Lauga, W. R. DiLuzio, G. M. Whitesides, H. A. Stone, *Biophys. J.* 90, 4004-12 (2006) "Swimming in circles: Motion of bacteria near solid boundaries".
 96. W. R. DiLuzio, L. Turner, M. Mayer, P. Garstecki, D. B. Weibel, H. C. Berg, and G. M. Whitesides, *Nature* 435, 1271-1274 (2005), "Escherichia coli swim on the right-hand side".
 97. Y. Wu, B. G. Hosu, and H. C. Berg, *PNAS* 108, 4147-4151 (2011), "Microbubbles reveal chiral fluid flows in bacterial swarms".
 98. E. Ben-Jacob, I. Cohen, O. Shochet, A. Tenenbaum, A. Czirók, and T. Vicsek, *Phys. Rev. Lett.* 75, 2899 (1995), "Cooperative Formation of Chiral Patterns during Growth of Bacterial Colonies".
 99. E. Ben-Jacob, O. Schochet, A. Tenenbaum, I. Cohen, A. Csirik, and T. Vicsek, "Generic modelling of cooperative growth patterns in bacterial colonies" *Nature* 368, 46-49 (2004).
 100. H. Levine, E. Ben-Jacob, E. Cohen, and W.-J. Rappel, *Proc. 45th IEEE Conference on Decision and Control*, p. 5073 (2006).
 101. N. H. Mendelson, *PNAS* 73, 1740-1744 (1976), "Helical growth of *Bacillus subtilis*: a new model of cell growth."
 102. A. Varma, M. A. de Pedro, and K. D. Young, *J. Bacteriol.* 189, 5692-5704 (2007), "FtsZ directs a second mode of peptidoglycan synthesis in *Escherichia coli*."
 103. L. F. Jones, R. Carballido-Lopez, and J. Errington, *Cell* 104, 913 (2001).
 104. S. Wang, L. Furchtgott, K. C. Huang, and J. W. Shaevitz, *PNAS* 109, E595-E604 (2012), "Helical insertion of peptidoglycan produces chiral ordering of the bacterial cell wall".
 105. R. M. Figge, A. V. Divakaruni, and J. W. Gober, *Molecular microbiology* 51, 1321-1332 (2004), "MreB, the cell shape-determining bacterial actin homologue, co-ordinates cell wall morphogenesis in *Caulobacter crescentus*".
 106. C. W. Wolgemuth, Y. F. Inclan, J. Quan, S. Mukherjee, G. Oster, M. A. Koehl, *Phys. Biol.* 2: 189199 (2005) "How to make a spiral bacterium".
 107. N. H. Mendelson, J. E. Sarlls, C. W. Wolgemuth, and R. E. Goldstein, "Chiral self-propulsion of growing bacterial macrofibers on a solid surface", *Phys. Rev. Lett.* 84 162730 (2000). Mendelson N H, Thwaites J J, Kessler J O and Li C 1995 *Mec*
 108. S. S. Andrews and A. P. Arkin, *Biophys. J.* 93, 1872-1884 (2007), "A mechanical explanation for cytoskeletal rings and helices in bacteria".
 109. J. Salje, F. van den Ent, P. de Boer, and J. Löwe, *Molecular cell* 43, 478-487 (2011), "Direct membrane binding by bacterial actin MreB".

Thank: S. van Teeffelen, N. S. Wingreen,